FCTUC DEPARTAMENTO DE ENGENHARIA CIVIL
FACULDADE DE CIÊNCIAS E TECNOLOGIA
UNIVERSIDADE DE COIMBRA

Structural behavior of hybrid lattice – tubular steel wind tower

Dissertação apresentada para a obtenção do grau de Mestre em Engenharia Civil na Especialidade de Mecânica Estrutural

Autor

Guilherme Gandolfi Figueiredo

Orientador

Professor Doutor Carlos Alberto da Silva Rebelo

Coimbra, Julho, 2013

AGRADECIMENTOS

Meus agradecimentos vão primeiramente a todos os meus amigos que me apoiaram nesta grande jornada. A todos os meus familiares, em especial aos meus pais, Maria Cecília Gandolfi Figueiredo e Joaquim Marques Figueiredo Neto, irmãos Felipe Gandolfi Figueiredo e Nathalia Gandolfi Figueiredo e afilhados Matteo Figueiredo Macorin e Anita Figueiredo Macorin, que sempre acreditaram e confiaram em mim, o meu profundo e sentido agradecimentos.

Gostaria também de mostrar o meu apreço ao Professor Doutor Carlos Alberto da Silva Rebelo pelo incentivo e orientação recebida, pela sua total disponibilidade e paciência ao longo de todo o caminho percorrido, o meu reconhecimento e gratidão.

RESUMO

O principal objectivo da presente proposta consiste em desenvolver uma nova solução híbrida em aço para torres de turbinas eólicas de multi - megawatt, utilizando uma estrutura em aço treliçada que servirá de suporte a parte superior da torre de secção tubular. A utilização de torres com secção tubular em aço na parte superior deve-se ao facto de aproveitar o conhecimento já estabelecido e optimizado dessa tecnologia, com diâmetros apropriados para serem transportados em estradas públicas. A parte treliçada da torre introduz a possibilidade de torres mais altas (além de seu custo de produção ser mais baixo) e utiliza um novo tipo de sistema de montagem para a secção tubular, através de um processo de deslizamento, por meio de macacos hidráulicos evitando assim a necessidade da utilização de grandes guindastes.

Importantes vantagens deste conceito são: (i) velocidade de construção, evitando o uso de grandes guindastes ou torres de elevação e da sua disponibilidade , (ii) o uso da tecnologia de torres de secção tubular já conhecida dos construtores de torres e perfeitamente estabelecida no mercado , (iii) optimização das fundações e da seção transversal da torre ao longo de toda a sua altura;

Palavras-chave: torre eólica híbrida / estrutura treliçada / ligações metálicas aparafusadas pré-esforçadas.

ABSTRACT

The main objective of this proposal is to develop a new hybrid steel solution for multi-megawatt wind turbine towers, using a steel lattice structure supporting a steel tubular upper part of the tower. The use of a tubular part takes advantage of the well-known and optimized technology of tubular steel towers with diameters suitable to be transported on public roads. The lattice part of the tower introduces the possibility of higher towers (than are economically feasible in tubular construction) and facilitates a new type of erection system for the tubular section by a sliding procedure, using hydraulics jacks, thus avoiding the need for very large cranes.

Important advantages of this concept are: (i) speed of construction, avoiding the use of expensive and availability-dependent large cranes or lifting towers, (ii) use of technology already established for tubular towers, (iii) optimization of foundation and tower cross section along height;

Keywords: hybrid wind tower / lattice structure / pre-stressed bolted steel connections.

Index

SYMBOLS

MW Megawatt

CO_2 Carbone dioxide

GW Gigawatt

m Meters

% Percentagem

mm Milimiters

fy Yield strength

fu Yield failure

E Elastic modulus

G Modulus of rigidit

υ Poisson coeficient

α Coeficient of linear thermal expansion

ρ Density

A Area

$W_{pl.}$ Plastic section modulus

$W_{el.}$ Elastic section modulus

I Second moment of inertia

i Radius of gyration about the relevant axis

I_T St. Venant torsional constant

γ_{Mi} Particular partial factor

M_{ed} Design bending moment

$M_{N,Rd}$ Design plastic moment resistance reduced due to the axial force N_{Ed}

$M_{pl,Rd}$ Bending plastic resistance

N_{ed} Design axial force

$N_{pl,Rd}$ Axial plastic resistance

$N_{c,Rd}$ Design resistance to normal forces of the cross-section for uniform compression

V_{ed} Share force design

$V_{pl,Rd}$ Plastic design shear resistance

χ_{LT} Reduction factor for lateral-torsional buckling

χ_i Reduction factor for relevant buckling mode

L_{Ei} Buckling length

A_v Shear area

$F_{v,Ed}$ The design shear resistance per bolt

$F_{s,Rd}$ The design slip resistance per bolt at the ultimate limit state

$F_{b,\ Rd}$ The design bearing resistance per bolt

$A_{net.}$ Net area of a cross section

A_{nt} Net area subjected to tension

A_{nv} Net area subjected to share

t_p The thickness of the plate under the bolt or the nut

h_p The length of the plate

e_1 The end distance from the centre of a fastener hole to the adjacent end of any part, measured in the direction of load transfer

e_2 The edge distance from the centre of a fastener hole to the adjacent edge of any part, measured at right angles to the direction of load transfer

d_0 The hole diameter for a bolt, a rivet or a pin

d The nominal bolt diameter, the diameter of the pin or the diameter of the fastener

$N_{t,Rd}$ Design values of the resistance to tension forces

p_1 The spacing between centres of fasteners in a line in the direction of load transfer

p_2 The spacing measured perpendicular to the load transfer direction between adjacent lines of fasteners *n* The number of the friction surfaces or the number of fastener holes on the shear face

ABBREVIATIONS

U.E.	União Europeia
2D	Two dimensions
3D	Three dimensions
EC0	Eurocode 0
EC1	Eurocode 1
EC2	Eurocode 2
EC3	Eurocode 3
EWG	Extreme Wind Model
EOG	Extreme Operating Gust Model

1 INTRODUCTION

1.1 Background

Global warming has become the most talked-about environmental issue today. Governments, corporations, and individuals around the world are debating the reality of global warming and possible solutions. Renewable energy technologies and efficient energy utilization are identified as the most effective potential solutions to these global challenging problems.

Renewable energy is the energy that comes from resources which are continually replenished such as sunlight, wind, waves, geothermal heat, etc. In 2007, about one-fifth of the global primary energy demand was met by renewable sources and the remainder by fossil fuels and nuclear energy. However, the largest share of renewable energy was attributable to biomass, primarily traditional biomass such as firewood and charcoal for cooking and heating. The rest was derived from large-scale hydropower or distributed among other renewable energy technologies - primarily biofuels, geothermal and wind power. In terms of electricity generation, renewable energy represented about 16 per cent, with non-hydro accounting for only a small fraction of that (UN-Energy, 2013).

Recently, a campaign promoted by the European Union (E.U.), called Europe 2020 Strategy, established that countries of U.E.-27 must reduce greenhouse gas emissions by 20% (or even 30%) as compared to 1990, produce 20% of energy from renewable sources and increase energy efficiency by 20%, all be reached in 20 years. The strategy responds to the challenges of reorienting policies away from crisis management and towards the introduction of medium-to-longer term reforms that promote growth and employment and ensure the sustainability of public finances.

By the end of 2011, the total power output generated using wind energy worldwide had increased, relative to 2010, by 20.6% to 238.351,0 MW (GWEC - Global Wind Energy Council, 2012). Although this increase was greatly influenced by new installations in China, and in spite of the financial crises, new installations in Europe-27 in that year maintained the same 9.6 GW attained in 2010. The European annual new installations of wind power have increased steadily over the last 17 years from 814 MW in 1995 to the maximum ever attained in 2009 of 10.5 GW corresponding to an annual average market growth of 15.6 % (EWEA - The European Wind Energy Association, February 2012).

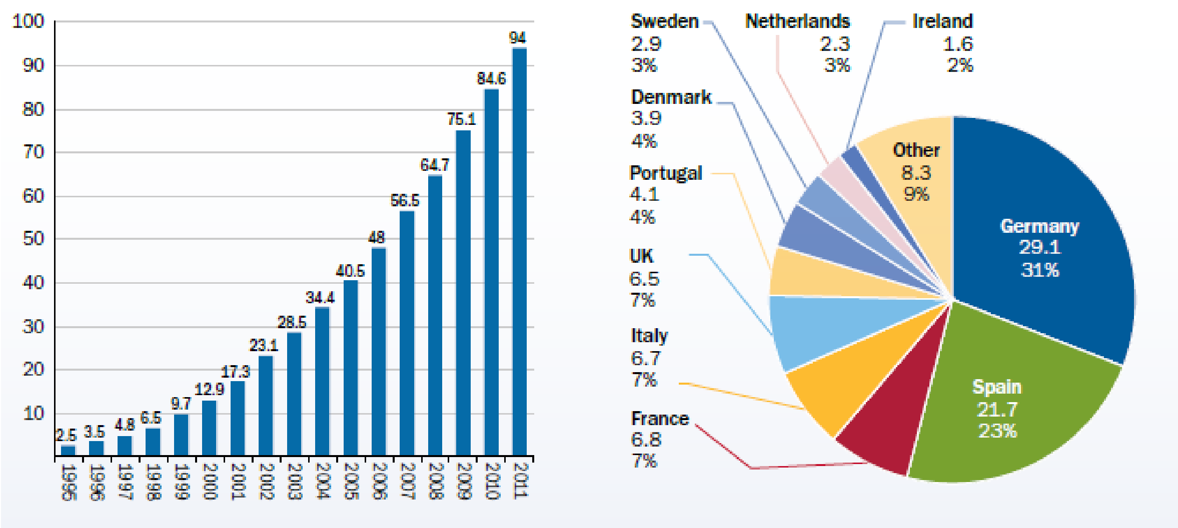

Figure 1: Cumulative wind power installations in the E.U. (GW); E.U. state market shares for total installed capacity at end 2011 (total 93.7 GW); source: (EWEA - The European Wind Energy Association, February 2012).

The evolution of wind turbine power over time shows that, in the last 20 years, turbines have grown from about 0.5 MW in capacity and 60 meters in hub height to around 7 MW and 160 meters hub height, although 2 to 5 MW turbines are still the most common. The mean power of the turbines installed in ten biggest onshore wind farms in Europe commissioned or under construction in 2012 was 2.6 MW. It is estimated that the average wind farm will have a turbine size of up to 10 MW by the year 2030 (Vattenfall, 2011).

However, it can be concluded that the more powerful is the turbine, the higher will be the tower and the greater its efficiency. The consequence of taller wind towers is the need to increase the structural strength and stiffness required to carry both increased turbine weight and bending forces under wind action on the rotors and the tower. For the current wind towers, mostly “Steel tubular towers”, this has implications on the assembly, high cost manufacturing and transportation.

According to (Hau,2006), the transportation and the erection procedures are developing into an increasing problem for the latest generation of multi-megawatt wind turbines. Tower heights of more than 100 m and tower head weights of several hundred tons require a diameter at the tower base of more than five meters; with the consequence that road transportation will no longer be feasible.

The high tower is an essential component of the horizontal-axis turbine, a fact which can be both an advantage and a disadvantage. The costs, which can amount to up to 20% of the overall turbine costs, are, of course, disadvantageous. As the height of the tower increases, transportation, assembly and erection of the tower and servicing of the components also become increasingly more difficult and costly. On the other hand, the specific energy yield of the rotor also increases with tower height. Theoretically, the optimum tower height lies at the point where the two growth functions of construction cost and energy yield intersect (Hau, 2006).

The competitiveness of wind energy was mainly achieved through the optimization of the construction process based on the use of tubular segments pre-fabricated and transported to the construction site to be assembled. It is now necessary that this concept must evolve in order to maintain competitiveness in future for higher steel towers.

1.2 Objectives

The aim of this thesis is to develop a new hybrid steel solution for multi-megawatt onshore wind turbine tower, using steel lattice structure supporting a steel tubular upper part of the tower. The use of a tubular part takes advantage of the well-know and optimized technology of tubular steel tower with diameters suitable to be transported on public roads. The lattice part of the tower introduces the possibility of higher towers, which are not economically feasible in tubular construction, and facilitates a new type of erection system for the tubular section by a slide procedure, thus avoiding the need for very large cranes.

The aim of this thesis is, first, the development of the concept based on the use of a lattice structure that supports the upper tubular part of the tower. The design of the lattice structure follows this concept and is done for the situation where a 5MW wind turbine is used. Furthermore, this design is done in accordance to the Structural Eurocodes, mainly Eurocode 3 (CEN, 2005) and to the international standard applied to wind tower design (IEC, 2005).

The initial design and structural analysis of the tower is performed using the computer software “Autodesk Robot Structural Analysis Professional 2012”. After performing an initial check of the natural frequencies of the tower, two types of design were performed: ultimate limit state and fatigue limit state. Finally, a numerical analysis of the optimized structure and the design of the joints allowed the assessment of structural safety.

1.3 Summary

The thesis is composed in six chapters:

Chapter 1 provides a briefing introduction of renewable energy and background of height wind towers. Also is presented the aim of this work thesis.

Chapter 2 addresses the state of art presenting the types of current wind towers, their advantages and disadvantages and its evolution.

In Chapter 3 a conceptual design model of lattice tower is presented and all design requirements considered are extensively discussed. A schematized mechanical model of transition piece including its boundary conditions, material and load condition is provided for structural analysis and numerical modeling purpose.

Chapter 4 presents the structural behavior of the tower. Three numerical models and respective analysis for ultimate limits states are presented and design results are discussed.

Chapter 5 presents the new cross-sections of the tower members and the conceptual design of the transition element. Also the optimization of the transition element and the optimized design of one type of connection are presented including detailed fatigue limit state check.

Finally, in Chapter 6 the conclusions and future work are addressed.

Cited references and relevant appendices are also attached.

2 STATE OF THE ART

2.1 The Tower

The first information about the existence of windmills from historical sources originated from the year 644 A.D. That is the oldest type of "wind turbines". These were low in height, in relation to the rotor diameter, and voluminous construction in accordance with their function as a work space, thus also providing for the necessary stiffness. The windmills were used for milling grain or pumping water. Soon, however, the advantage of increased height was recognized and the millhouses became more slender and more tower-like. But it is only in modern-day constructions, first in the small American wind turbines and then later in the first power-generating wind power stations, that "masts" or "towers" were used, the sole function of which lay in supporting the rotor and the mechanical components of the tower head (Hau, 2006). The tower of a wind turbine supports the nacelle and the rotor and provides the necessary elevation of the rotor to keep it clear off the ground and bring it up to the level where the wind resources are.

As a consequence of the development, designs and materials for towers increased in variety. Steel and concrete took the place of the wood construction of the millhouses. In the early years of the development of modern wind energy technology, the most varied tower designs were tried out and tested but in the course of time, the range has been narrowed down to free-standing designs, mainly of steel and more rarely of concrete (Hau, 2006).

2.2 Lattice Tower

The steel lattice structures are a very well-known technology for building a range of tower types, such as for energy transmission lines, and they were even used to support wind turbines at the beginning of wind energy exploitation.

In the initial years of commercial wind energy utilization, lattice towers were widely used in small turbines. As their sizes increased, steel tubular towers increasingly displaced the lattice towers. Recently, the interest in lattice towers has been rekindled, particularly in connection with large turbines with a hub height of 100m and more (Hau, 2006).

The advantages of the use of lattice towers are:

- Straightforward design and detailing;
- Good dynamic behavior (ideal for wind turbines);
- Economy of transportation (lattice angle sections are easier and lighter to transport when compared to tubular structures);
- Simpler erection procedures;

The much longer assembly time on site and the greater expenditure for maintenance are considered as disadvantages of lattice towers.

2.3 Concrete Tower

The wind industry’s identified need for increased turbine sizes, rotor diameters and tower heights makes concrete a competitive option. Concrete can offer tall, strong, sophisticated wind farm structures for onshore or offshore deployment in aggressive marine or remote inland environments which require durable materials.
Concrete is an inherently durable material capable of maintaining its desired engineering properties under conditions of extreme exposure. Concrete’s constituent materials can easily be tailored to economically provide different degrees of durability depending on exposure, environment and the properties desired. Another advantage of concrete towers is its dynamic performance. As concrete has an inherently higher damping property than other materials, solutions with less noisy and vibration are deliverable. This is beneficial in terms of not only structural demands such as fatigue failure, but also public acceptance issues in relation to the noise emission.

Concrete allows very high towers to be built without being associated with unsolvable transport problems. The long construction period, too, can be shortened today by means of various methods of using prefabricated parts (Hau, 2006).

2.4 Steel Tubular Tower

Most of the wind power towers are tubular steel structures. According to a periodical published by (Elforsk, 2012), the advantages of tubular towers are:

- Tubular steel structure is relatively light and due to its circular cross section has the same bending stiffness in all direction;
- Has god torsional stiffness;
- Required natural frequency can easily be achieved for certain types of turbines and hub heights;
- It is relatively easy to install and has low maintenance costs.

As previously mentioned, development of turbines with higher maximum power, increased hub height and increased steel price has made the steel tower less economical. Increased hub height decreases the natural frequency of the structure. Furthermore, increased wind power, i.e. turbine power, increases the loads, bending and torsional moments acting on the structure. In order to withstand the increased loadings the dimensions of the tower must be increased, i.e. both diameter of the tube and the thickness of the plate and tube wall must be increased, which lead to further implications, namely transportation (Elforsk, 2012). As this will require larger cross sectional diameters, the increased size may introduce significant transportation problems, bearing in mind that 4.5m is the practical limit for the diameter of complete ring sections that can be transported along the public highway.

3 CONCEPTUAL MODEL OF THE LATTICE SEGMENT

The structural analysis of the lattice tower can only be possible after understanding all the requirements that this structure should meet. After the outcome of a conceptual design model, further analysis and adjustment can be made in order to ensure every detailed requirement.

3.1 Design Requirements

After a brief presentation of different types of wind towers, this thesis has dedicated to give an integrated view on the feasibility of optimizing the performance of onshore hybrid steel wind tower with 150m high hub. The hybrid wind tower is composed by 50m of 3D lattice tower (superstructure), which will support the main steel tubular tower structure with 100m height hub and a 5 MW wind turbine on the top.

The lattice tower has been designed to provide stiffness and robustness. To achieve that, the superstructure was conceived to be compact, with a global ratio slenderness equal one, with 25m as the base radius. The truss action and larger base dimensions of the tower help resist the applied loads more effectively leading to a lighter structural design.

The superstructure consists of eight legs, with one leg diameter and thickness. Connected by new tubular steel cross-section through pre-stressed bolting, the legs are attached with the bracing members forming a vertical plane frame or truss, type Pratt or N. The legs are inclined 66^{o} from the ground and they are positioned in a circle. To provide more stiffness in the top of the tower, the distance among the truss braces decrease, allowing the lattice tower to become a strength structure. The layout of the truss leads a K-joint angle for the whole structure.

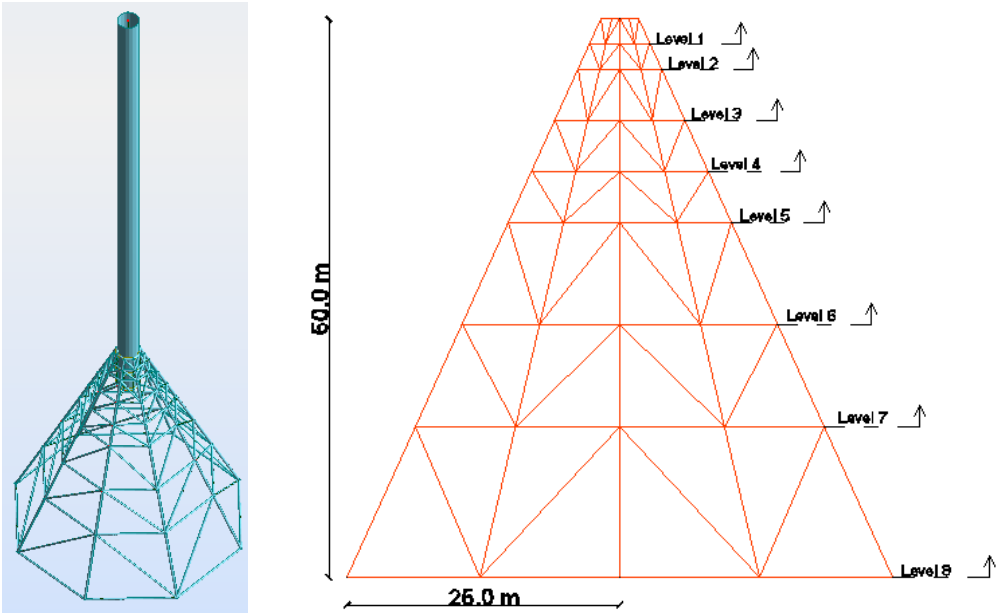

(a) (b)

Figure 2: a) The conceptual model of hybrid lattice-tubular steel wind tower; (b) Outline drawings of the tower.

The new tubular cross-section consists in bolted separate parts, with different layout and dimensions, feasible to be easily transported and assembled in-site. The main priorities of new tubular cross-section are: the reduction of connections costs, fatigue design limitations and use of "almost" maintenance-free fasteners. The design and manufacturing of bolted connections are developed for the effective in-site assembling of lattice tower part while considering the extensive use of maintenance free pre-stressed bolts.

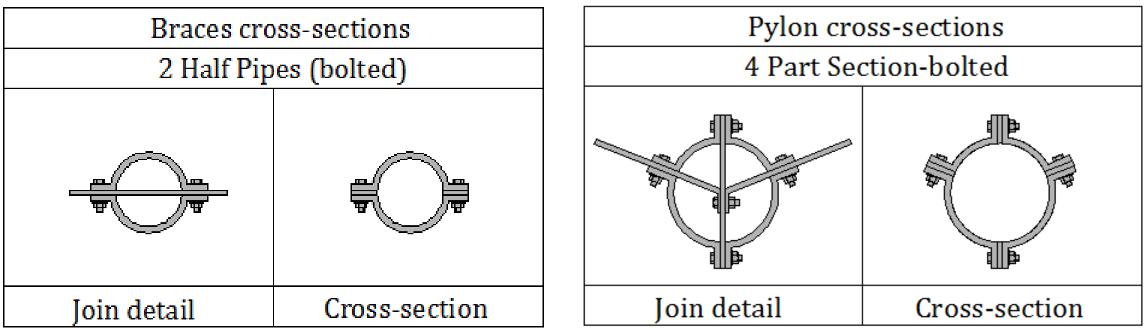

(a) (b)

Figure 3: New cross-section; a) braces section; b) Legs section.

An important part of the structure, responsible with transmitting all efforts of the steel tubular tower to the superstructure, is the transition piece. The transition piece cross-section consists in eight section-bolted parts, forming flanges that are connected by gusset plate on the lattice tower. Its geometry is 4500mm of diameter and is composed by two pipes overlapped, each one with 4560mm height.

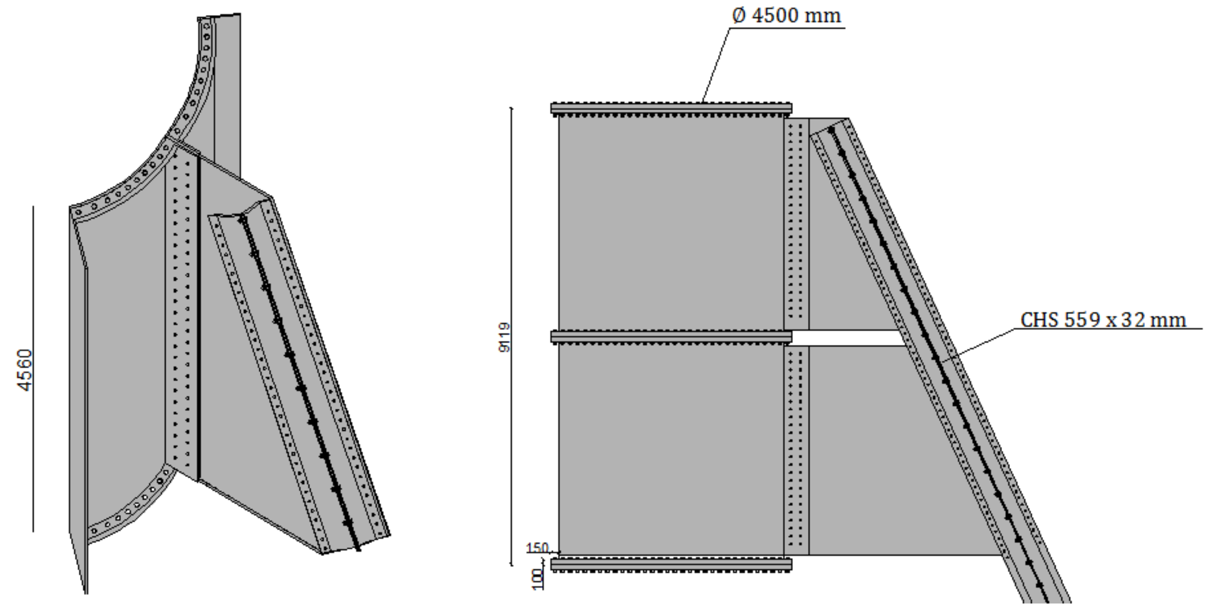

(a) (b)

Figure 4: a) 1/8 of one segment of transition piece; b) Two segments overlapped linking CHS 559 x 32mm by a gusset plate.

3.2 Material

The properties of the steel used on the structural design, S355NH/NLH, fulfill all ductility requirements established by the EC3 Part 1-1, section 3 (CEN, 2005a). The nominal values of yield strength "*fy*" and ultimate strength "*fu*" steel is defined according to standard EN 10210-1 (CEN, 1994), and in general are obtained as characteristic values, as displaced on table 1.

fy (N/mm^2)	355.0
fu (N/mm^2)	490.0
E (N/mm^2)	210000.0
G (N/mm^2)	81000.0
υ	0.3
α (^{o}C^{-1})	12x10^{-6}
ρ (Kg/m^3)	7850.0

Table 1: Material properties of the lattice tower.

In respect of joint design, the properties of the steel of pre-loaded bolts are established on EC3 part 1-8, section 1.2.4 Reference standards: Group 4. According to EC3-1-8 section 3 (CEN, 2005b) "only bolts assemblies of class 8.8 and 10.9 conforming to the requirements given in section 1.2.4 Reference standards: Group 4 for High Strength Bolting for pre-loading with controlled tightening in accordance with the requirements in 1.2.7 Reference Standards: Group 7 may be used as pre-loaded bolts". The bolts class chosen for this study was class 10.9 and for the other components of joints the class of steel chosen is S355 JR (CEN, 2005a; CEN, 2004b).

Bolts class	4.6	4.8	5.6	5.8	6.8	8.8	10.9
fyb (N/mm^2)	240	320	300	400	480	640	900
fub (N/mm^2)	400	400	500	500	600	800	1000

Table 2: Nominal values of the yield strength *fyb* and the ultimate tensile strength *fub* for bolts.

Hollow section	S355 NH/NHL
Bolts	Class 10.9
Joint components	S355 JR

Table 3: Summarize material properties.

3.3 Mechanical Model of Superstructure

Based on previous description of conceptual design requirements for the lattice tower in terms of the geometry and power utilities layout, a mechanical model of the tower can be simplified as following for engineering modeling and structural analysis.

3.3.1 Design Loads and Combinations

The loads cases and the partial safety factors which were obtained (Carlos Rebelo, 2012) based on Eurocode 1 (CEN, 2002). This document performed research on wind class II-A turbines, the most common wind class turbine in use. This research was based on wind loads acting directly on tower and the effects of wind acting on the rotor during operation, represented by concentrated loads on the top of the tower. For ultimate limit state, three design situations are considered:

- The extreme non-operation condition (EWM)
- The extreme operation condition (EOG)
- Fatigue condition

Therefore, the load table (table 4) for the three different situations was prepared based on $V_{ref.}$ = 42.5 m/s and $I_{ref.}$ = 15 m/s ($V_{ref.}$ is the reference of wind velocity at hub height obtained from the extreme of 10 minutes of average of wind speed measurements and $I_{ref.}$ is the expected value of the turbulence intensity) (Carlos Rebelo, 2012).

Wind Load	**EWM**	**EOG**
Fx_{top} (KN)	578	1065
Fy_{top} (KN)	578	1065
Fz_{top} (KN)	-5000	-4879
Mx_{top} (KN.m)	28568	14987
My_{top} (KN.m)	28568	14987
Mz_{top} (KN.m)	5834	3966

Table 4: 5 MW wind turbine – 150m, values not combined.

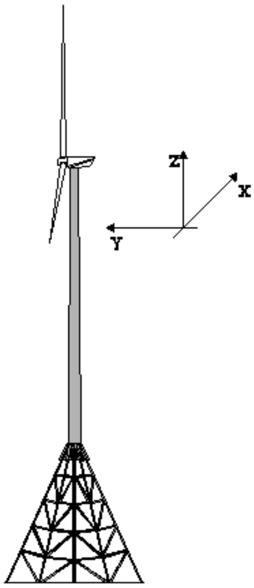

Figure 5: Coordinate system used for the design of wind turbines.

On table 5 the damage equivalent load ranges, for fatigue limit state, are given for the parameters m =3 and $N_{ref} = 2.0$ E8, which are obtained from the 20 years life-time.

ΔFx (KN)	203
ΔMx (KN.m)	781
ΔMy (KN.m)	4065
ΔMz (KN.m)	3950

Table 5: Damage equivalent loads for m = 3 and $N_{ref.} = 2.0 \times 10^8$.

The combination of actions is based on EN1990, section 6.4.3.2 (CEN, 2001) where established the fundamental combination for Ultimate Limit State:

$$N_{Ed} = \sum_{j\geq 1} \gamma_{G,J} G_{k,j} \text{ "+" } \gamma_P P \text{ "+" } \gamma_{Q,1} Q_{k,1} \text{ "+" } \sum_{i>1} \gamma_{Q,i} \Psi_{0,i} Q_{k,i} \qquad \text{(Eq.3.1)}$$

The partial safety factors for loads are given in Table 6.

Unfavorable loads	1.35
Favorable loads	0.90
Fatigue loads	1.00

Table 6: Partial safety factors for loads.

3.3.2 The Conceptual Model

Structural analysis during optimization process is performed using the software "Autodesk Robot Structural Analysis Professional 2012". As previously described, the model is a hybrid lattice-tubular tower composed by 100m height hub steel tubular tower and 50m lattice tower. The steel tubular tower is an element-column with 4500mm of diameter and 30mm of thickness. On this model, is in charge of transmission of efforts (bending moments and axis forces) and its own weight, to the lattice tower. The transmission of efforts is performed by the transition piece, which is represented in the model by three rings with high level of stiffness connected by a "rigid link", as demonstrated in figure 6.

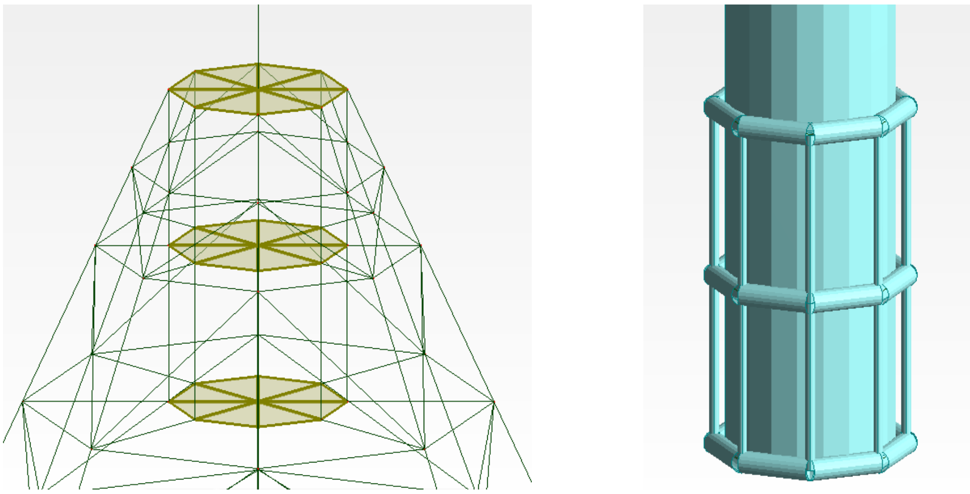

(a) (b)

Figure 6: a) Rigid link; b) Transition piece modeling.

The lattice tower is connected with the transition piece by element-bars, which are released to avoid the transmission of bending moments and it only transfers the axis forces. However, all elements bars of the superstructure are released which allows to work as a truss structure. The modeling is performed using the following profiles (table 7):

Chords or Pylons	CHS 559 x 32 mm
Braces	CHS 406.4 x 32 mm
Horizontal bars	CHS 406.4 x 32 mm

Table 7: Modeling structural components profile.

Taking into account the constructability issues and for better overview of the optimization process, the elements of the superstructure is divided into eight groups based on their location and dimensions (see figure 2).

Group nº	Location - element (length)
1	Level 1 – chords (2.5 m); braces (3.38 m); horizontal bars (2.70 m)
2	Level 2 – chords (2.5 m); braces (3.96 m); horizontal bars (3.48 m)
3	Level 3 – chords (5.0 m); braces (6.53 m); horizontal bars (5.06 m)
4	Level 4 – chords (5.0 m); braces (7.65 m); horizontal bars (6.63 m)
5	Level 5 – chords (5.0 m); braces (8.90 m); horizontal bars (8.20 m)
6	Level 6 – chords (10.0 m); braces (13.90 m); horizontal bars (11.34 m)
7	Level 7 – chords (10.0 m); braces (16.25 m); horizontal bars (14.48 m)
8	Level 8 – chords (14.83 m); braces (22.30 m); horizontal bars (19.14 m)

Table 8: Groups and locations of the structural elements.

3.3.3 Boundary Conditions

The lower boundary condition is conceived to allow the tower the “splash movement” avoiding the bending moments in the base. The support model consists in a fixed constraint in the Z direction, (vertical, Figure 7) and a slide system in the X and Y direction (horizontal) allowing the movement of the lattice support structure in the respective direction. Actually, those directions need to be represented by a springs with bending stiffness of foundation, which demands a depth study, and that is not contemplated on this work. The connecting legs were released in the bases to avoiding the transition of bending moment to the foundation and bracing bars are introduced in the base to ensure the locking of the tower.

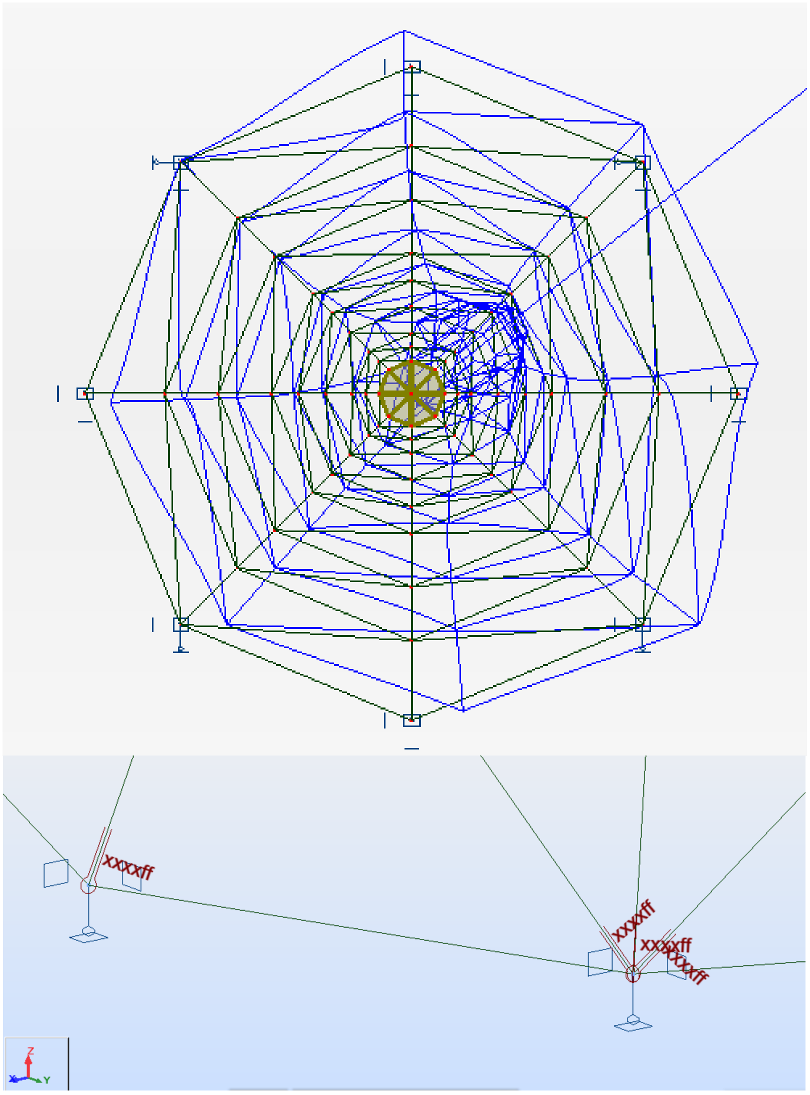

Figure 7: Top image: “splash” displacement – top view; Bottom image: Slade support system.

4 STRUCTURAL ANALYSIS AND DESIGN OF THE LATTICE TOWER

This project has been developed according with the general requirements of EC 3 part 1-1 (CEN, 2005a). "Its complies with the principles and requirements for the safety and serviceability of structures, the bases of their design and verification that are given in EN 1990 (CEN, 2001) – Bases of structural design".

On standard EN 1990 is established that structural safety is ensured by use of a safety class methodology. The structure to be designed is classified into a safety class based on the failure consequences. The classification is normally determined by the purpose of the structure. As the structural design is according to EC3 (CEN, 2005a), it can be adopted a reliability differentiation class RC2, established in (CEN, 2001), which the factor for actions is K_{FI} = 1.0.

4.1 Structural Analysis

The capacity of the elements resistance of a structure is not relevant if the design efforts are not adequately evaluated. The overall analysis of efforts and displacements in a structure, and in particular a metal frame, essentially depends on the characteristics of deformability and stiffness. However, the global stability and the local stabilities of their elements, the behavior of the cross sections and of joints, the imperfections and deformability of support also depends on deformability and stiffness. Thus, the definition of the kind of analysis to adopt a particular situation should be taken into account all aspects.

To determine what kinds of structural analysis adopt on this case, a study of 2D structure is performed (Providência, 2008), as showed the following outline:

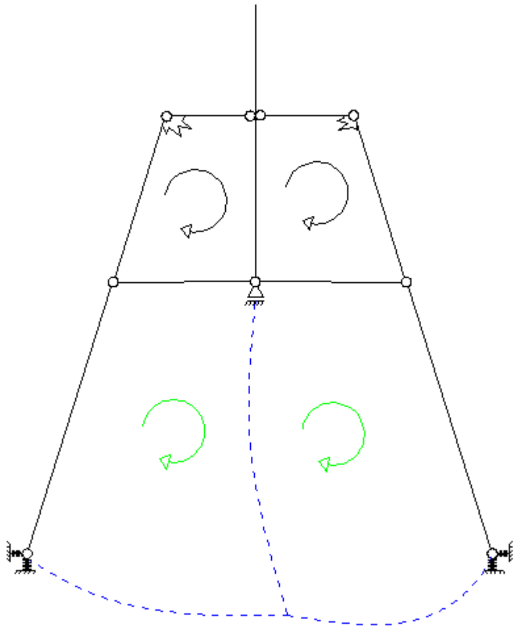

Figure 8: 2D outline of the hybrid-lattice tower.

$$\alpha = 3(m_{ext.} + m_{int.}) - (l_{ext.} + l_{int.}) = 3(2 + 2) - (4 + 8) = 0; \qquad \text{(Eq. 4.1)}$$

$$\alpha = 0 \rightarrow \text{isostatic structure}$$

where, α is the statically indeterminate degree;

$m_{ext.}$ is the external net;

$m_{int.}$ is the intern net;

$l_{ext.}$ is the external degree freedom;

$l_{int.}$ is the intern degree freedom;

As an isostatic structure a global linear elastic analysis is performed.

The design of steel structures normally leads to optimized structures and consequently quite slender. Potentially, the phenomena of instability increases with the slenderness of the elements, and it is normally necessary to check the global stability of the structure. Therefore, the legs are studied, initially, as a global element, because the stability on direction z (see figure 9), out of the plane frame is a critical point, since on direction y (plane frame) they are locked by the braces. The global verification forces a second order analysis (method 2), with consideration of imperfections. According to EC3 part 1-1, section 5.2.1 (2) (CEN, 2005a) the effects of the deformed geometry (second-order effects) should be considered if they increase the action effects significantly or modify significantly the structural behavior. On section 5.2.1 (3), first order analysis may be used for the structure, if the increase of the relevant internal forces or moments or any other change of structural behavior caused by deformations can be neglected. This condition may be assumed to be fulfilled, if the following criterion is satisfied:

$$\alpha_{cr} = \frac{F_{cr}}{F_{ed}} \geq 10 \quad \text{for elastic analysis;} \qquad \text{(Eq.4.2)}$$

where, α_{cr} is the factor by which the design loading would have to be increased to cause elastic instability in a global mode;

F_{ed} is the design loading on the structure;

F_{cr} is the elastic critical buckling load for global instability mode based on initial elastic stiffnesses;

The results has showed that the values of α_{cr} are lower than 10, and nonlinear buckling analysis has to be considered.

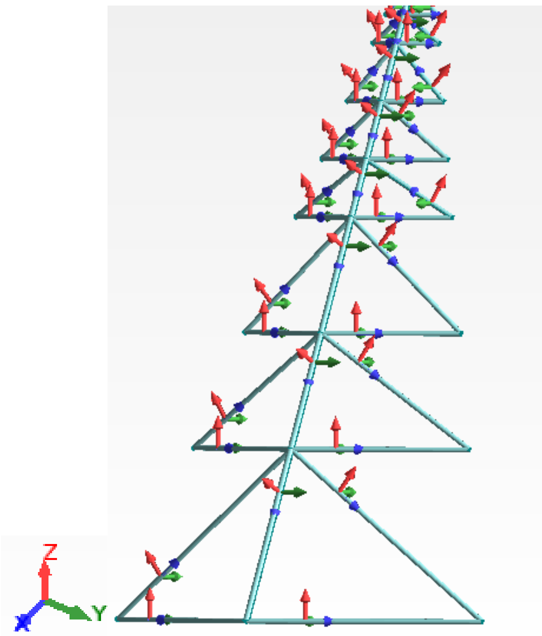

Figure 9: Local coordinates system of legs and braces.

As mentioned in chapter 3, the top of the tower is the segment with greater stiffness on tower due to the high level of bending moment transmission from the steel tubular tower. Therefore, as shown on figure 10, the top displacements are bigger than other segments and the bending of the tower is the most important mode shape. As it can be seen on figure 10, the displacements of the lattice tower are small, which can be concluded that the structure is a rigid element capable of tolerating all efforts transmitted. Another important conclusion about the displacements of the tower is the leg's buckling length. As we can see in figure 11, due to the sinusoidal deformity of the legs, the buckling length can be adopted as a distance between joints, and the local stability analysis is performed.

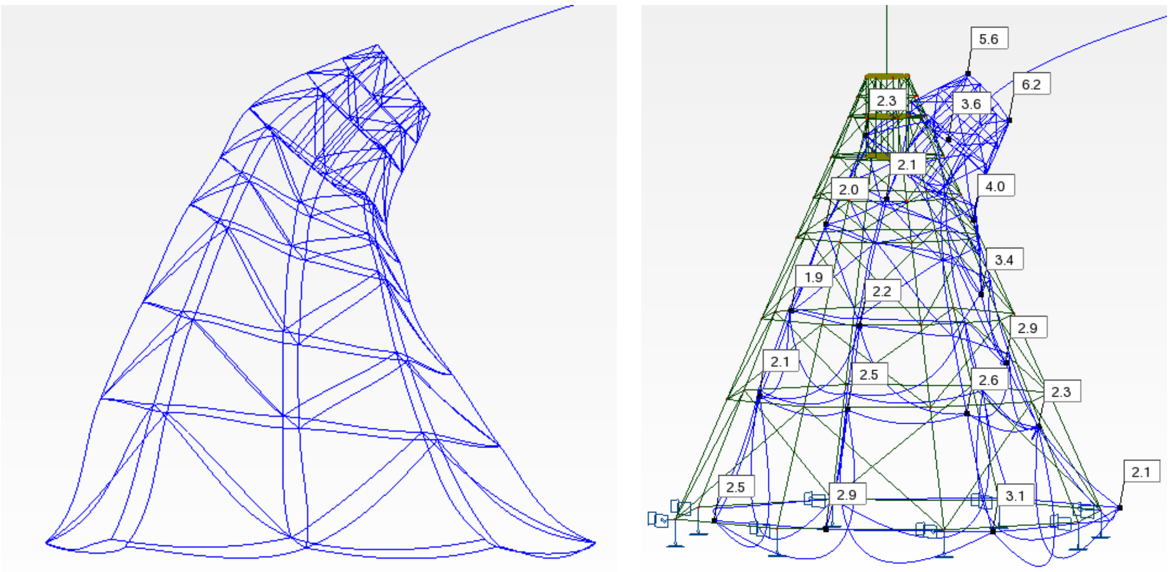

(a) (b)

Figure 10: (a) First mode shape (α_{cr} = 2.0); (b) Displacements with second order effects

4.1.1 Ultimate Limit State

The design process is in accordance with the EC3-1-1, section 5 (CEN, 2005a) where it is established that, the "second order effects and imperfections may be accounted partially by the global analysis and partially through individual stability checks of members according to section 6.3 (Buckling resistance of members)". As mentioned on chapter 3.3 of this thesis, the design efforts are obtained by ultimate limit state combinations and all verifications are based on the envelope failure, as demonstrate on figures 11, 12 and 13 (Local coordinate system, figure 9).

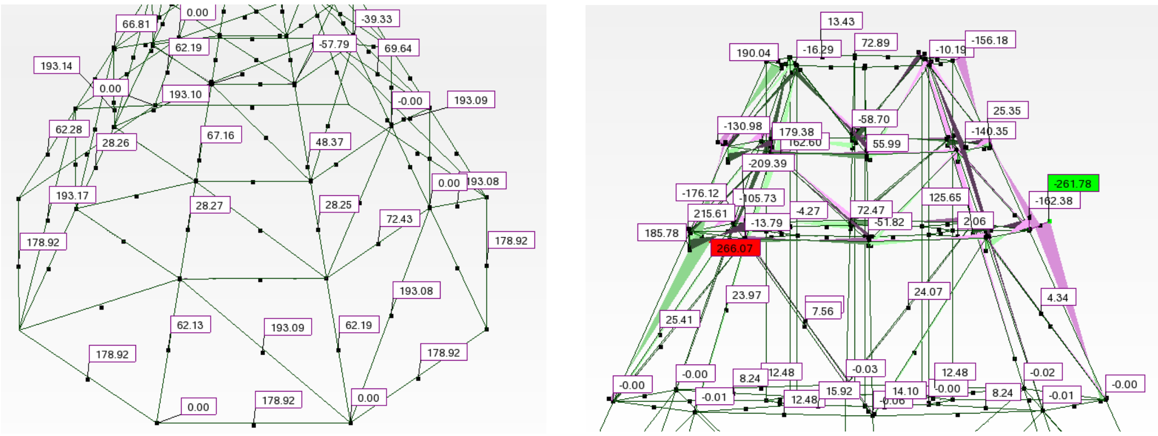

Figure 11: Diagram of bending moments (My); Left image: Bottom the tower; Right image: Top the tower

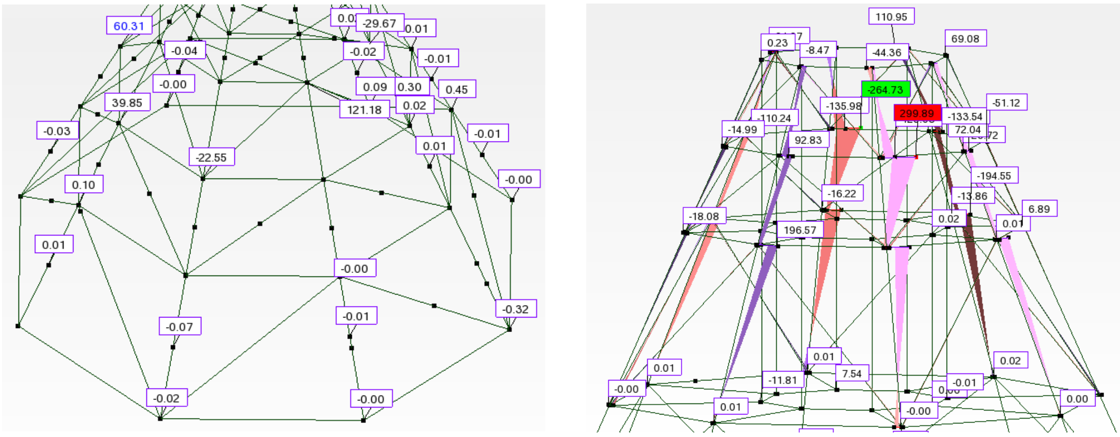

Figure 12: Diagram of bending moment (Mz); Left image: Bottom the tower; Right image: Top the tower

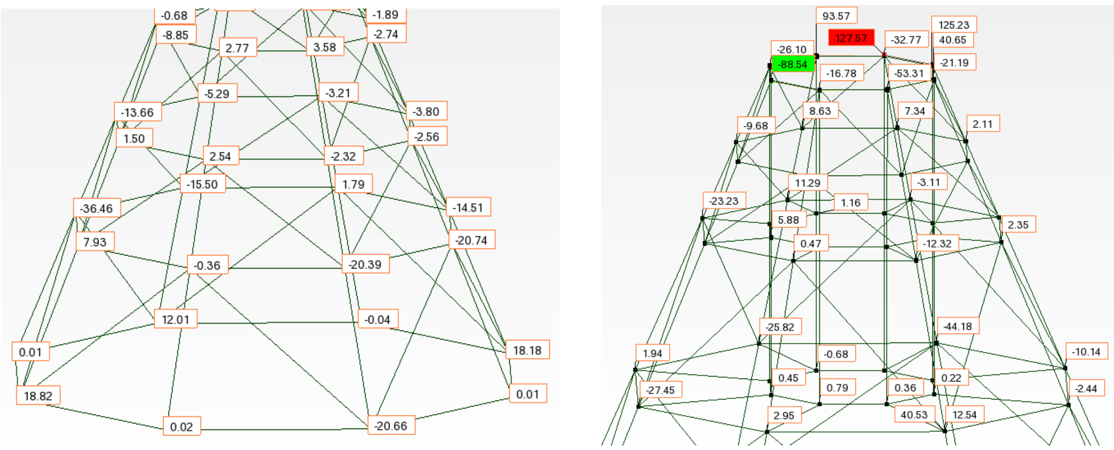

Figure 13: Diagram of torsion moment (Mx); Left image: Bottom the tower; Right image: Top the tower

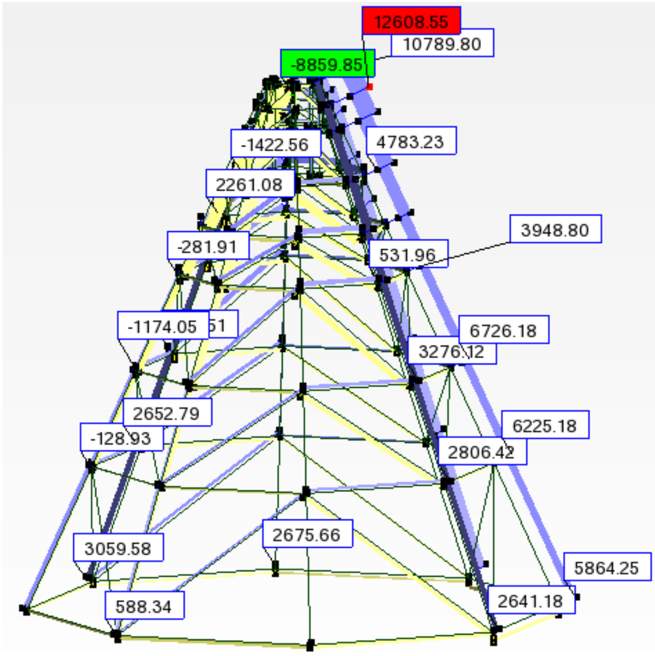

Figure 14: Diagram axis force (Fx)

As previously mentioned and it can be observed that, the top of the tower is the segment of the structure that retain the all bending moment transmitted from the steel tubular tower, that's the reason to confer it a high level of stiffness by the chords and braces, decreasing the distance between then. Other observation is, due the releases introduced in the model, the bottom segment of the tower works as a truss structure, transmitted only axis forces and residual bending moments until the foundation (see figure 11 to 13). As is observed on figure 14, all horizontal bars on bottom of tower is working on tension (yellow diagram), blocking the displacements and locking the legs.

With an intention to validate the results and a better overview from the optimization process, a numerical analysis is performed.

4.1.2 Numerical Analysis

For validation of results, is chosen three elements to be studied, a chord on group 3 (see table 8), which is the element most on bending in the top; from group 8, a brace on bottom of the tower, which is the most slender element; and from group 8, a chord, which is the most on compression element. First example is the chord (CHS 559 x 32mm) on top, with 5.0m length. As mentioned on previous section, the design process demonstrated bellow, is based on envelope failure efforts, obtaining the extreme values for design. On software “Autodesk Robot Structural Analysis Professional 2012” the element is divided in 11 parts, is studied the worst situation and the process is optimized.

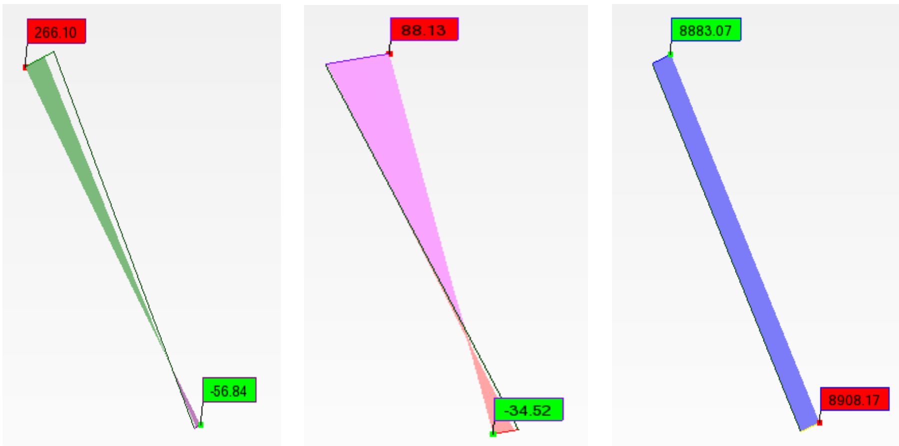

(a) (b) (c)

Figure 15: Diagram of efforts (U.L.S); a) Bending moments (My); b) Bending moments (Mz); c) Axis forces (Fx).

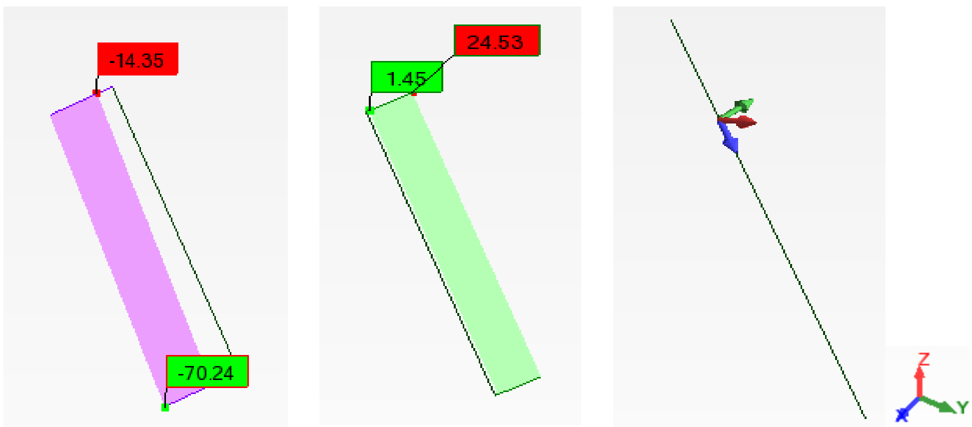

(a) (b) (c)

Figure 16: Diagram of efforts (U.L.S); a) Shear forces (Fz); b) Shear forces (Fy); c) Local coordinate system.

A (cm^2)	529.5
$W_{pl,y}$ (cm^3)	8898.0
$W_{el,y}$ (cm^3)	6605.0
I_y (cm^4)	184510.0
i_y (cm)	18.7
$W_{pl,z}$ (cm^3)	8898.0
$W_{el,z}$ (cm^3)	6605.0
I_z (cm^4)	184510.0
i_z (cm)	18.7
I_T (cm^4)	369207.0

Table 9: Geometry properties - CHS 559 x 32mm.

E (N/mm^2)	210000.0
fy (N/mm^2)	355.0

Table 10: Steel Properties (see chapter 3).

The partial factors γ_{Mi} is defined on EC3-1-1, section 6.1 (CEN, 2005a), and the following numerical values are recommended:

γ_{M0}	1.00
γ_{M1}	1.00
γ_{M2}	1.25

Table 11: Partial factors in National Annex Portuguese.

The design process starts on the verification of cross-section requirements, according EC3-1-1 section 5.5 (CEN, 2005a), as expressed in equation 4.3.

Tubular sections

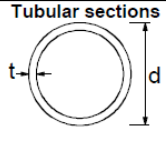

Class	Section in bending and/or compression
1	$d/t \leq 50\varepsilon^2$
2	$d/t \leq 70\varepsilon^2$
3	$d/t \leq 90\varepsilon^2$ **NOTE** For $d/t > 90\varepsilon^2$ see EN 1993-1-6.

$\varepsilon = \sqrt{235/f_y}$	f_y	235	275	355	420	460
	ε	1,00	0,92	0,81	0,75	0,71
	ε^2	1,00	0,85	0,66	0,56	0,51

Figure 17: Maximum width-to-thickness ratios for compression parts; **source**: EC3-1-1

$$\frac{d}{t} = \frac{559}{32} \cong 17.5 \leq 50 * 0.66 = 33 \text{ (class 1)} \qquad \text{(Eq. 4.3)}$$

As the class of the cross-section is class 1, the verification of the cross-section resistance is based on plastic design. According EC3-1-1, section 5.4.2 (2) (CEN, 2005a), "Internal forces and moments may be calculated according elastic global analysis even if the resistance of a cross section is based on its plastic resistance". Next step is section bending resistance, considering a bi-axial bending force, EC3-1-1, section 6.2.9 (CEN, 2005a).

$$\left[\frac{M_{y,Ed}}{M_{N,y,Rd}}\right]^{\alpha} + \left[\frac{M_{Z,Ed}}{M_{N,z,Rd}}\right]^{\beta} \leq 1 \qquad \text{(Eq. 4.4)}$$

in which, α and β are constants; α = 2 and β = 2;

where, $M_{N,i,\,Rd}$ is the design plastic moment resistance reduced due to the axial force $N_{Ed;}$

$$M_{N,y,Rd} = M_{N,z,Rd} = M_{pl,Rd}(1 - n^{1.7}) = 3158.80 \times (1 - 0.474^{1.7}) = 2270.9 \qquad \text{(Eq. 4.5)}$$

$$M_{pl,Rd} = fy \times W_{pl} = 355 \times 10^{3} \times 8898 \times 10^{-6} = 3158.8 \text{ KNm}$$

$$n = \frac{N_{Ed}}{N_{pl,Rd}} = \frac{8909}{18798.32} = 0.474$$

$$N_{pl,Rd} = \frac{A\, f_y}{\gamma_{M0}} = \frac{529.53 \times 10^{-4} \times 355 \times 10^{3}}{1.0} = 18798.3 \text{ KN}$$

$$\left[\frac{266.1}{2270.94}\right]^{2} + \left[\frac{88.13}{2270.94}\right]^{2} = 0.015 < 1.0 \text{ OK!!}$$

The plastic shear forces resistances are verified as EC3-1-1 section 6.2.6 (CEN, 2005a).

$$\frac{\mathrm{V_{Ed}}}{\mathrm{V_{pl,Rd}}} \leq 1.0 \qquad \text{(Eq. 4.6)}$$

$$\mathrm{V_{pl,Rd}} = \frac{\mathrm{A_v}\left(\frac{\mathrm{fy}}{\sqrt{3}}\right)}{\gamma_{\mathrm{M0}}} = \frac{0.034 \times \left(\frac{355 \times 10^3}{\sqrt{3}}\right)}{1.0} = 6968.6 \text{ KN} \qquad \text{(Eq. 4.7)}$$

$$A_\mathrm{v} = \frac{2A}{\pi} = \frac{2 \times 529.53 \times 10^{-4}}{\pi} = 0.034 \text{ m}^2$$

$$\frac{70.24}{6968.62} = 0.01 \leq 1.0 \text{ OK!!}$$

The plastic compression resistance is verified according EC3-1-1 section 6.2.4 (CEN, 2005a).

$$\frac{\mathrm{N_{Ed}}}{\mathrm{N_{c,Rd}}} \leq 1.0 \qquad \text{(Eq. 4.8)}$$

$$\mathrm{N}_{c,Rd} = \frac{A\,f_y}{\gamma_{M0}} = \frac{529.5 \times 10^{-4} \times 355.0 \times 10^3}{1.0} = 18798.3 \text{ KN} \qquad \text{(Eq. 4.9)}$$

$$\frac{\mathrm{N_{Ed}}}{\mathrm{N_{c,Rd}}} = \frac{8908.2}{18798.3} = 0.5 \leq 1.0 \text{ OK!!}$$

The interaction between bending and shear forces has to be verified according the EC3-1-1, section 6.2.10 (CEN, 2005a), but as we can see above the applied shear forces is low and it can be waived.

After the study of the plastic resistance of the cross-section, an important and crucial point is the stability verification of the element (method 2). As a hollow cross-section, due the high level stiffness of lateral torsional buckling, its verification may be waived.

The elements which are subjected to combined bending and axial compression
should satisfy (CEN, 2005a):

(Eq. 4.10)

$$\frac{N_{Ed}}{\frac{\chi_y N_{Rk}}{\gamma_{M1}}} + k_{yy}\frac{M_{y,Ed}}{\chi_{LT}\frac{M_{y,Rk}}{\gamma_{M1}}} + k_{yz}\frac{M_{Z,Ed}}{\frac{M_{Z,Rk}}{\gamma_{M1}}} \leq 1.0$$

$$\frac{N_{Ed}}{\frac{\chi_z N_{Rk}}{\gamma_{M1}}} + k_{zy}\frac{M_{y,Ed}}{\chi_{LT}\frac{M_{y,Rk}}{\gamma_{M1}}} + k_{yz}\frac{M_{Z,Ed}}{\frac{M_{Z,Rk}}{\gamma_{M1}}} \leq 1.0 \qquad \text{(Eq. 4.11)}$$

where, N_{Ed}, $M_{y,Ed}$ and $M_{z,Ed}$ are the design values of the compression force and the maximum moments about the y-y and z-z axis along the member, respectively.

χ_y and χ_z are the reduction factors due to flexural buckling from 6.3.1.

χ_{LT} is the reduction factor due to lateral torsional buckling from 6.3.2.

k_{yy}, k_{yz}, k_{zy}, k_{zz} are the interaction factors.

The resistances characteristics of cross-section (CHS559 x 32 mm) are given by:

$$N_{Rk} = A \times fy = 529.5 \times 10^{-4} \times 355.0 \times 10^{3} = 18798.3 \text{ KN}$$

$$M_{y,Rk} = M_{z,Rk} = W_{pl} \times fy = 8898.0 \times 10^{-6} \times 355.0 \times 10^{3} = 3158.8 \text{ KNm}$$

Reduction factors are calculated according EC3-1-1, section 6.3 (CEN, 2005a):

<u>Plane x-z (see figure 16 - c):</u>

$L_{E,y}$ = 5.0m (On EC3-1-1, Annex BB.1.3, is suggested that $L_{E,i}$ for chords equal $L_{E,i}$ = 0.9 L, but on this case study is adopted $L_{E,I}$ = 1.0 L).

$$\overline{\lambda_y} = \frac{L_{E,y}}{i_y} \times \frac{1}{\lambda_1} = \frac{5}{18.7 \times 10^{-2}} \times \frac{1}{76.4} = 0.35 \qquad \text{(Eq. 4.11)}$$

$$\lambda_1 = \pi\sqrt{\frac{E}{\sigma_c}} = \pi\sqrt{\frac{210000}{355}} = 76.4 \qquad \text{(Eq. 4.12)}$$

α = 0.21 - curve a; hot finished; S355; EC3-1-1, section 6.3, table 6.2 (CEN, 2005a)

$$\emptyset = 0.5\left[1 + \alpha(\bar{\lambda} - 0.20) + \bar{\lambda}^2\right] = 0.5\,[1 + 0.21\,(0.35 - 0.20) + 0.35^2] \cong 0.6 \qquad \text{(Eq. 4.13)}$$

$$\chi_y = \frac{1}{\emptyset + \sqrt{\emptyset^2 - \bar{\lambda}^2}} = \frac{1}{0.6 + \sqrt{0.6^2 - 0.35^2}} = 0.96 \qquad \text{(Eq. 4.14)}$$

Plane x-y:

$L_{E,z} = 5.0$ m

$$\overline{\lambda_z} = \frac{L_{E,z}}{i_{yz}} \times \frac{1}{\lambda_1} = \frac{5}{18.7 \times 10^{-2}} \times \frac{1}{76.4} = 0.35$$

$$\lambda_1 = \pi\sqrt{\frac{E}{\sigma_c}} = \pi\sqrt{\frac{210000}{355}} = 76.4$$

α = 0.21 - curve a; hot finished; S355; EC3-1-1, section 6.3, table 6.2 (CEN, 2005a)

$$\emptyset = 0.5\left[1 + \alpha(\bar{\lambda} - 0.20) + \bar{\lambda}^2\right] = 0.5\,[1 + 0.21\,(0.35 - 0.20) + 0.35^2] = 0.58$$

$$\chi_z = \frac{1}{\emptyset + \sqrt{\emptyset^2 - \bar{\lambda}^2}} = \frac{1}{0.58 + \sqrt{0.58^2 - 0.35^2}} = 0.96$$

As a section not susceptible to torsional deformations, the interaction factors are obtained as demonstrates on table 12 (EC3-1-1, Annex B, table B.1):

K_{yy}	$C_{my}\left(1+(\bar{\lambda}_y-0.2)\frac{N_{ed}}{\chi_y\frac{N_{Rk}}{\gamma_{M1}}}\right)\leq C_{my}\left(1+0.8\frac{N_{Ed}}{\chi_y\frac{N_{Rk}}{\gamma_{M1}}}\right)$	(Eq. 4.15)
K_{yz}	$0.6\ K_{zz}$	(Eq. 4.16)
K_{zy}	$0.6\ K_{yy}$	(Eq. 4.17)
K_{zz}	$C_{mz}\left(1+(\bar{\lambda}_z-0.2)\frac{N_{Ed}}{\chi_z\frac{N_{Rk}}{\gamma_{M1}}}\right)\leq C_{mz}\left(1+0.8\frac{N_{Ed}}{\chi_z\frac{N_{Rk}}{\gamma_{M1}}}\right)$	(Eq. 4.18)

Table 12: Interaction factors k_{ij} for members not susceptible to torsional deformations.

Where the equivalent uniform moment factor C_{mij} are obtained according table 13:

Moment diagram	range		C_{my} and C_{mz} and C_{mLT} uniform loading	C_{my} and C_{mz} and C_{mLT} concentrated load
 M, ψM	$-1 \leq \psi \leq 1$		$0,6 + 0,4\psi \geq 0,4$	$0,6 + 0,4\psi \geq 0,4$
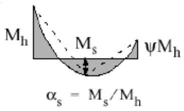 M_h, M_s, ψM_h; $\alpha_s = M_s/M_h$	$0 \leq \alpha_s \leq 1$	$-1 \leq \psi \leq 1$	$0,2 + 0,8\alpha_s \geq 0,4$	$0,2 + 0,8\alpha_s \geq 0,4$
	$-1 \leq \alpha_s < 0$	$0 \leq \psi \leq 1$	$0,1 - 0,8\alpha_s \geq 0,4$	$-0,8\alpha_s \geq 0,4$
		$-1 \leq \psi < 0$	$0,1(1-\psi) - 0,8\alpha_s \geq 0,4$	$0,2(-\psi) - 0,8\alpha_s \geq 0,4$
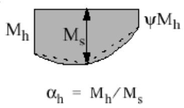 M_h, M_s, ψM_h; $\alpha_h = M_h/M_s$	$0 \leq \alpha_h \leq 1$	$-1 \leq \psi \leq 1$	$0,95 + 0,05\alpha_h$	$0,90 + 0,10\alpha_h$
	$-1 \leq \alpha_h < 0$	$0 \leq \psi \leq 1$	$0,95 + 0,05\alpha_h$	$0,90 + 0,10\alpha_h$
		$-1 \leq \psi < 0$	$0,95 + 0,05\alpha_h(1+2\psi)$	$0,90 - 0,10\alpha_h(1+2\psi)$

For members with sway buckling mode the equivalent uniform moment factor should be taken $C_{my} = 0,9$ or $C_{Mz} = 0,9$ respectively.

C_{my}, C_{mz} and C_{mLT} should be obtained according to the bending moment diagram between the relevant braced points as follows:

moment factor	bending axis	points braced in direction
C_{my}	y-y	z-z
C_{mz}	z-z	y-y
C_{mLT}	y-y	y-y

Table 13: Equivalent uniform moment factors C_{mij}; **source:** EC3-1-1.

$C_{my} = 0.9$ (elements with sway buckling mode on direction z)

$$C_{mz} = 0.6 + 0.4 \times \Psi_z \geq 0.4 = 0.6 + 0.4 \times -0.392 = 0.443 \qquad \text{(Eq. 4.19)}$$

$$M_{z,Ed,top} = 88.13\ \text{KNm};\quad M_{z,Ed,bottom} = -34.52\ \text{KNm};\quad \Psi_z = \frac{M_{z,Ed,bottom}}{M_{z,Ed,top}} = \frac{-34.52}{88.13} = -0.392;$$

<u>K_{yy} (see equation 4.15):</u>

$$K_{yy} = 0.9 \left[1 + (0.4 - 0.2) \frac{8908.2}{0.96 \left(\frac{18798.3}{1.0} \right)} \right] = 0.967$$

$$\text{with, } K_{yy} = 0.967 < 0.9 \left[1 + 0.8 \frac{8908.2}{0.96 \left(\frac{18798.3}{1.0} \right)} \right] = 1.3 \rightarrow K_{yy} = 0.967$$

K_{yz} (see equation 4.16):

$K_{yz} = 0.6 \text{ x } 0.476 = 0.286$

K_{zz} (see equation 4.18):

$$K_{zz} = 0.443 \left[1 + (0.35 - 0.2) \frac{8908.2}{0.96 \left(\frac{18798.3}{1.0} \right)} \right] = 0.476$$

$$\text{with, } K_{zz} = 0.476 < 0.443 \left[1 + 0.8 \frac{8908.2}{0.96 \left(\frac{18798.3}{1.0} \right)} \right] = 0.618 \rightarrow K_{zz} = 0.476$$

K_{zy} (see equation 4.17):

$K_{zy} = 0.6 \text{ x } 0.967 = 0.58$

$\chi_{LT} = 1.0$ (As a hollow cross-section, there is no lateral buckling)

$$\frac{8908.17}{0.96 \left(\frac{18798.32}{1.0} \right)} + 0.967 \frac{266.10}{1.0 \left(\frac{3158.79}{1.0} \right)} + 0.286 \frac{88.13}{\left(\frac{3158.79}{1.0} \right)} = 0.58 \leq 1.0 \quad \text{OK!!}$$

$$\frac{8908.17}{0.96 \left(\frac{18798.32}{1.0} \right)} + 0.580 \frac{266.10}{1.0 \left(\frac{3158.79}{1.0} \right)} + 0.476 \frac{88.13}{\left(\frac{3158.79}{1.0} \right)} = 0.56 \leq 1.0 \quad \text{OK!!}$$

Next element to be verified is the brace (CHS 406.4 x 32mm) on bottom of the tower with 22.30 (see table 8, group 8), which is the most slender element. The efforts are characterized by bending moment and axial force.

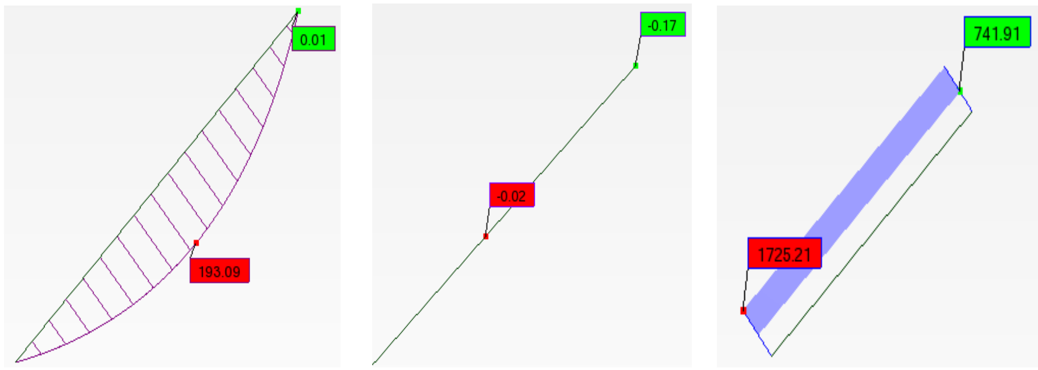

(a) (b) (c)

Figure 18: Diagram of efforts; a) Bending moment (My); b) Bending moment (Mz); c) Axial forces.

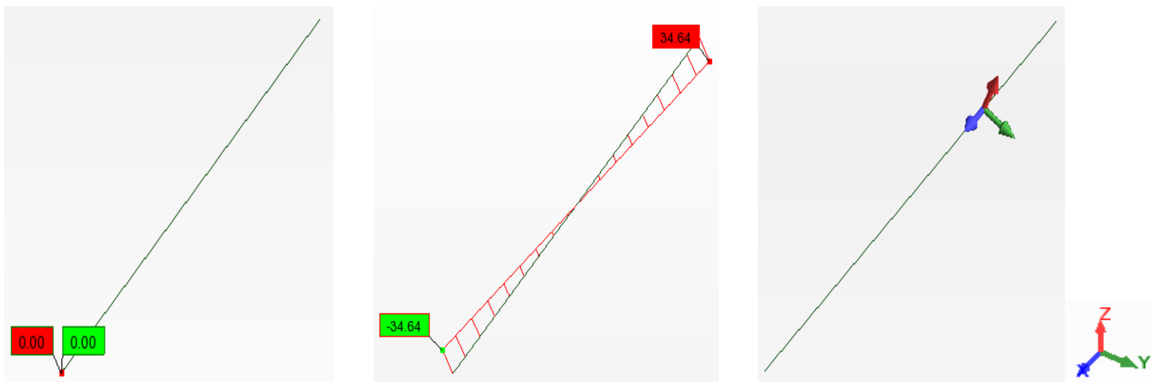

(a) (b) (c)

Figure 19: Diagram of efforts; a) Shear force (Fy); b) Shear force (Fz); c) Local coordinate system.

A (cm^2)	376.0
$W_{pl,y}$ (cm^3)	4497.0
$W_{el,y}$ (cm^3)	3269.0
I_y (cm^4)	66430.0
i_y (cm)	13.3
$W_{pl,z}$ (cm^3)	4497.0
$W_{el,z}$ (cm^3)	3269.0
I_z (cm^4)	66430.0
i_z (cm)	13.30
I_T (cm^4)	132900.0

Table 14: Geometry properties - CHS 406.4 x 32mm.

E (N/mm^2)	210000.0
fy (N/mm^2)	355.0

Table 15: Steel properties.

Similar the element studied before, the following study is based on EC3-1-1 (CEN, 2005a)

- Cross-section requirements: (see Equation 4.3)

$$\frac{d}{t} = \frac{406.4}{32.0} \cong 12.7 \leq 50 * 0.66 = 33.0 \text{ (class 1)}$$

- Resistance of cross-section:

Bending moments and axial forces:

$$M_{N,y,Rd} = M_{N,z,Rd} = M_{pl,Rd}(1 - n^{1.7}) = 1596.4\ (1 - 0.129^{1.7}) = 1547.3 \text{ KN}$$

$$M_{pl,Rd} = f_y \times W_{pl.} = 355.0 \times 10^3 \times 4497.0 \times 10^{-6} = 1596.4 \text{ KNm}$$

$$n = \frac{N_{ed}}{N_{pl,Rd}} = \frac{1725.2}{13348.0} = 0.129$$

$$N_{pl,Rd} = \frac{A\ f_y}{\gamma_{M0}} = \frac{376 \times 10^{-4} \times 355 \times 10^3}{1.0} = 13348.0 \text{ KN}$$

$$\frac{M_{Ed}}{M_{N,Rd}} = \frac{193.1}{1547.3} = 0.13 \leq 1.0 \text{ OK!!}$$

Shear forces resistance:

$$V_{pl,Rd} = \frac{A_v\left(\frac{f_y}{\sqrt{3}}\right)}{\gamma_{M0}} = \frac{0.024 \times \left(\frac{355 \times 10^3}{\sqrt{3}}\right)}{1.0} = 4919.0 \text{ KN}$$

$$A_v = \frac{2A}{\pi} = \frac{2 \times 376.0 \times 10^{-4}}{\pi} = 0.024 \text{ m}^2$$

$$\frac{V_{Ed}}{V_{Rd}} = \frac{34.6}{4919.0} = 0.007 \leq 1.0 \text{ OK!!}$$

Compression resistance:

$$N_{c,Rd} = \frac{A\, f_y}{\gamma_{M0}} = \frac{376.0 \times 10^{-4} \times 355.0 \times 10^3}{1.0} = 13348.0 \text{ KN}$$

$$\frac{N_{Ed}}{N_{c,Rd}} = \frac{1725.2}{13348.0} = 0.129 \leq 1.0 \text{ OK!!}$$

- <u>Buckling resistance of members</u>:

$$N_{Rk} = A \text{ x } fy = 376.0 \text{ x } 10^{-4} \text{ x } 355.0 \text{ x } 10^3 = 13348.0 \text{ KN}$$

$$M_{y,Rk} = M_{z,Rk} = W_{pl} \text{ x } fy = 4497.0 \text{ x } 10^{-6} \text{ x } 355.0 \text{ x } 10^3 = 1596.4 \text{ KNm}$$

<u>Plane x-z; Plane x-y (see figure 19 - c):</u>

$L_{E,y} = L_{E,z} = 22.30$ m

$$\overline{\lambda_y} = \overline{\lambda_z} = \frac{L_E}{i} \times \frac{1}{\lambda_1} = \frac{22.30}{13.3 \times 10^{-2}} \times \frac{1}{76.4} = 2.2$$

$$\lambda_1 = \pi \sqrt{\frac{E}{\sigma_c}} = \pi \sqrt{\frac{210000}{355}} = 76.4$$

$\alpha = 0.21$ - curve a; hot finished; S355; EC3-1-1, section 6.3, table 6.2 (CEN, 2005a)

$$\emptyset = 0.5\left[1 + \alpha\left(\overline{\lambda} - 0.20\right) + \overline{\lambda}^2\right] = 0.5\,[1 + 0.21\,(2.19 - 0.20) + 2.19^2] = 3.1$$

$$\chi_y = \chi_z = \frac{1}{\emptyset + \sqrt{\emptyset^2 - \overline{\lambda}^2}} = \frac{1}{3.11 + \sqrt{3.11^2 - 2.19^2}} = 0.2$$

C_{my} = 0.9 (elements with sway buckling mode on direction z)

<u>K_{yy} (see equation 13):</u>

$$K_{yy} = 0.9\left[1 + (2.19 - 0.2)\frac{1725.21}{0.188\left(\frac{13348.00}{1.0}\right)}\right] = 2.1$$

$$\text{with, } K_{yy} = 2.1 < 0.9\left[1 + 0.8\frac{1725.21}{0.188\left(\frac{13348.00}{1.0}\right)}\right] = 1.4 \rightarrow K_{yy} = 1.4$$

K_{zy} = 0 (On hollow sections under axial compression and uniaxial bending $M_{y,Ed}$; EC3-1-1, Annex B).

$$\frac{1725.2}{0.2\,\frac{13348.0}{1.0}} + 1.4\,\frac{193.2}{1.0\,\frac{1596.4}{1.0}} = 0.85 \leq 1.0 \text{ OK!!}$$

$$\frac{1725.2}{0.2\,\frac{13348.0}{1.0}} = 0.68 \leq 1.0 \text{ OK!!}$$

The last element to be studied is the chord (CHS 559 x 32mm) on the bottom of tower. The verification is based on the diagram presented below. The diagram has showed that element is working only in compression, and the bending moments is too low and it can be unvalued, as it can be seen on figure 20.

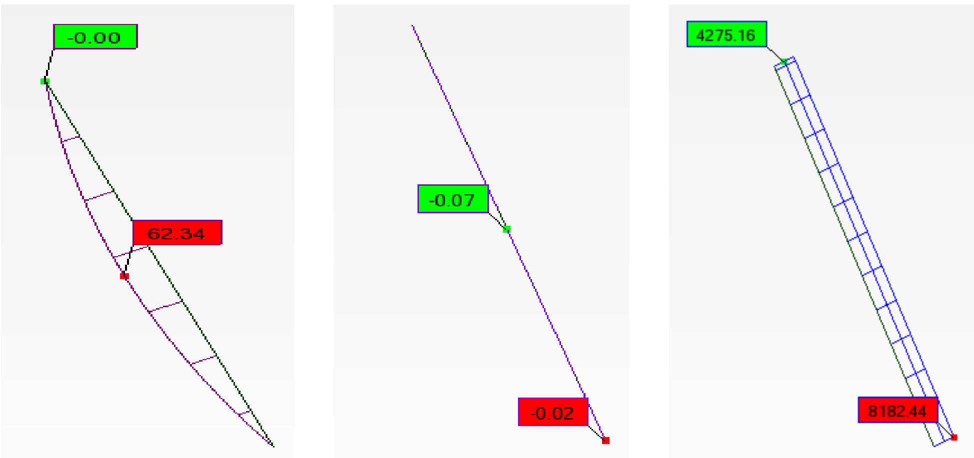

(a) (b) (c)

Figure 20: Diagram of efforts; a) Bending moment (My); b) Bending moment (Mz); c) Axial forces (Fx).

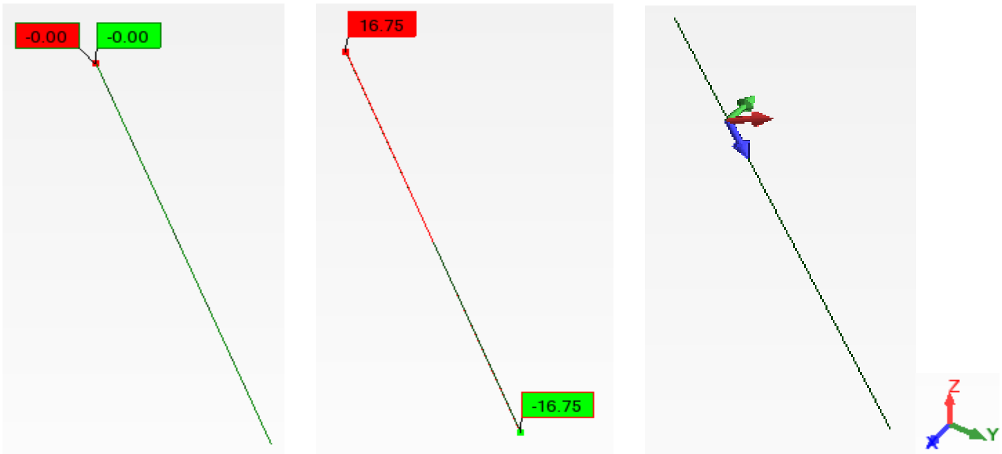

(a) (b) (c)

Figure 21: Diagram of efforts; a) Shear force (Fy); b) Shear force (Fz); c) Local coordinate system.

A (cm^2)	529.5
$W_{pl,y}$ (cm^3)	8898.0
$W_{el,y}$ (cm^3)	6605.0
I_y (cm^4)	184510.0
i_y (cm)	18.7
$W_{pl,z}$ (cm^3)	8898.0
$W_{el,z}$ (cm^3)	6605.0
I_z (cm^4)	184510.0
i_z (cm)	18.7
I_T (cm^4)	369207.0

Table 16: Geometry properties - CHS 559 x 32mm.

E (N/mm^2)	210000.0
fy (N/mm^2)	355.0

Table 17: Steel properties.

➢ Cross-section requirements: (see equation 4.3)

$$\frac{d}{t} = \frac{559.0}{32.0} \cong 17.5 \leq 50 \times 0.66 = 33.0 \text{ (class 1)}$$

➢ Resistance of cross-section:

Compression resistance:

$$N_{c,Rd} = \frac{A\, f_y}{\gamma_{M0}} = \frac{529.5 \times 10^{-4} \times 355.0 \times 10^{3}}{1.0} = 18798.3 \text{ KN}$$

$$\frac{N_{Ed}}{N_{c,Rd}} = \frac{8183.4}{18798.0} = 0.5 \leq 1.0 \text{ OK!!}$$

➢ Buckling resistance of members:

$$N_{Rk} = A \text{ x } fy = 529.5 \text{ x } 10^{-4} \text{ x } 355.0 \text{ x } 10^{3} = 18798.3 \text{ KN}$$

Plane x-z; Plane x-y (see figure 21 - c):

$L_{E,y} = L_{E,z} = 14.83$ m

$$\overline{\lambda_y} = \overline{\lambda_z} = \frac{L_E}{i} \times \frac{1}{\lambda_1} = \frac{14.8}{18.7 \times 10^{-2}} \times \frac{1}{76.4} = 1.1$$

$$\lambda_1 = \pi \sqrt{\frac{E}{\sigma_c}} = \pi \sqrt{\frac{210000}{355}} = 76.4$$

α = 0.21 - curve a; hot finished; S355; EC3-1-1, section 6.3, table 6.2 (CEN, 2005a)

$$\emptyset = 0.5\left[1 + \alpha(\bar{\lambda} - 0.20) + \bar{\lambda}^2\right] = 0.5\,[1 + 0.21\,(1.04 - 0.20) + 1.04^2] = 1.13$$

$$\chi_y = \chi_z = \frac{1}{\emptyset + \sqrt{\emptyset^2 - \bar{\lambda}^2}} = \frac{1}{1.13 + \sqrt{1.13^2 - 1.04^2}} = 0.6$$

$$\frac{8182.4}{0.6\,\frac{18798.3}{1.0}} = 0.7 \leq 1.0 \text{ OK!!}$$

$$\frac{8182.4}{0.63\,\frac{18798.3}{1.0}} = 0.7 \leq 1.0 \text{ OK!!}$$

4.1.4 Conclusions

In the previous section, an analysis of structural static behavior for ultimate limit state is performed. As an isostatic structure, a global linear analysis is considered. The lattice tower is a rigid structure, with a top rigid segment to care out the high level transmission of efforts from the steel tubular tower. The study of the first mode of shape, which is the bending of the tower, allowed a better approach of study, comprehending the behavior of the structure members. It's important to mention that the optimization process is restrained by a global analysis, becoming the elements less slender, and obtaining a local design ratio not too much optimized.

Element	**Ratio**
Chord – Level 3	0.58
Brace – Level 8	0.85
Chord – Level 8	0.70

Table 18: Local Ratio design values.

5 JOINTS AND TRANSITION ELEMENT

As mentioned on chapter 2, the new tubular cross-section consists in bolted separate parts, with different layout and dimensions, feasible to be easily transported and assembled in-situ. The main priorities of new tubular cross-section are reduction connections costs, fatigue design limitations and use of “almost” maintenance-free fasteners. Design and manufacturing of bolted connections developed for effective in-situ assembling of lattice tower part considering extensive use of pre-stressed bolts free of maintenance. All members of the lattice tower (chords, braces and horizontal braces) and the connections are composed by the conceptual cross-section.

This chapter is separated in three parts; the first is destined for the link of cross-section elements; the second part is addresses for K-joint, which connecting the braces and chord (see figure 24); and the third part is addresses for the conceptual transition piece that connects the lattice tower with steel tubular tower. Finally, a numerical analysis is performed for K-joint.

5.1 Link of Cross-Section Elements

As mentioned before, the members of the lattice tower are composed by the new cross-section, which will allow easiness assembly and transportations. The sections are composed by two parts on the braces (CHS 406.4 x 32mm) and by three parts on the legs (CHS 559 x 32mm) and they are linked by pre-stressed bolts, spaced by 0.50m from each other. Between the parts, exist a “fillet of steel”, with 30mm of thickness, that is responsible to ensure the level of the element until the connection, and to link the element among long elements, for example the braces of level 8, which is the slender element, with 22.30m. The fillet link two element with 10.15m, as it can be seen on figure 22.

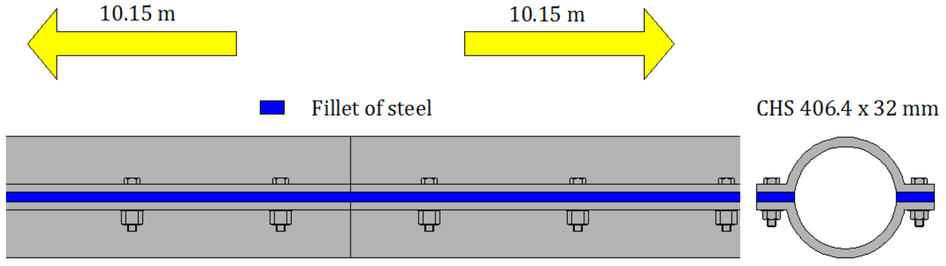

Figure 22: Fillet steel on CHS 406.4 x 32mm.

The elements on compression, the legs for example, the parts of new cross section only need a "soft grip" to be in touch, being the distance established sufficient to ensure the link. But on elements on share forces applied, the design of bolts should be according the EC3-1-8 (CEN, 2005b) for bolts subjected of share loads. Anyway, a brief approach of the verification is performed for extremes values of U.L.S. The element that is verified is a horizontal brace on level 2, with 2.70m length.

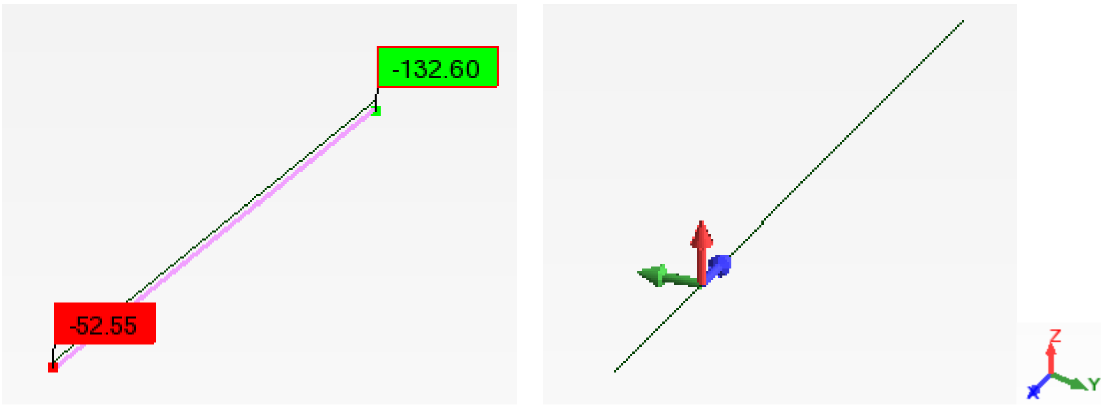

(a) (b)

Figure 23: a) Diagram of share force U.L.S. – CHS 406.4 x 32mm (Fz); b) Coordinate local system.

The bolts are classified as class C, and the criteria for verification are demonstrated on table 19 of next section. On this section only is performed the first criteria, the Slip – resistance, EC3-1-8, section 3.9 (CEN, 2005b)

Bolts Properties	
Type	M30
Area (mm^2)	561.0
Class	10.9
fu (N/mm^2)	1000.0

Table 19: Bolts properties.

$$F_{V,Ed} \leq F_{s,Rd} \quad \text{(Eq. 5.1)}$$

$$F_{p,Cd} = \frac{0.7\, f_{ub}\, A_s}{\gamma_{M7}} \quad \text{(Eq. 5.2)}$$

$$F_{p,Cd} = \frac{0.7 \times 1000 \times 10^3 \times 561 \times 10^{-6}}{1.1} = 357 \text{ KN (preload)}$$

$$F_{s,Rd} = \frac{k_s\, \eta\, \mu}{\gamma_{M3}} F_{p,c} \quad \text{(Eq. 5.3)}$$

where, K_s is the coefficients for normal hole (K_s = 1.0);

η is the number of friction surface (see figure 22);

μ is the slip factor (μ = 0.50);

$$F_{s,Rd} = \frac{1.0 \times 2.0 \times 0.5}{1.25} \times 357.0 = 286.0 \text{ KN (one bolt)}$$

$$F_{V,Ed} = 132.0 \text{ KN} \leq F_{s,Rd} = 286.0 \text{ KN OK!!}$$

As it can be seen, only one bolt is necessary to ensure the link of two parts of the CHS 406.4 x 32mm section, and the distance of 0.50m between bolts is enough to ensure the safety.

5.2 K-joint

A structural joint is a device formed by several components (welds, bolts, rivets, plates, etc.) ensuring the continuity and the transmission of efforts over structure. As described on chapter 3, section 3.2, the elements of lattice tower are released avoiding the transmission of bending moments and transmitting axial forces, working as a plane frame. The layout of chords and braces leads a “K-joint” angle for the whole structure. The angles between the chords and the brace members, and between adjacent brace members, should be not less than 30^o (CEN, 2005b). The K-joint is characterized by simple joint and composed by 4 parts of new cross-section (CHS 559 x 32mm), three gusset plate, which are connected between the flanges and by themselves, and pre-stressed bolted, as demonstrated on figure 23.

On this connection each component has a function. The gusset plate functions are transference of axial forces from the braces to the legs, transfer the share forces from the diagonal braces to the legs, and resist the tension forces cause by the braces. The flanges of the new cross-sections have the important task to be the component which link the element braces with the gusset plate, ensuring the transference of efforts, for it its important ensure ductility. Other important components are the bolts. On K-joint, the bolts are only subjected by shear loads, when are connected the flanges of CHS 406.4 x 32mm with gusset plate and when are connected the gusset plate with the flanges of CHS559 x 32mm. On the link of gusset plates, exist a component of tensile load and component of share load, but that are residual loads and it can be neglected (see figure24).

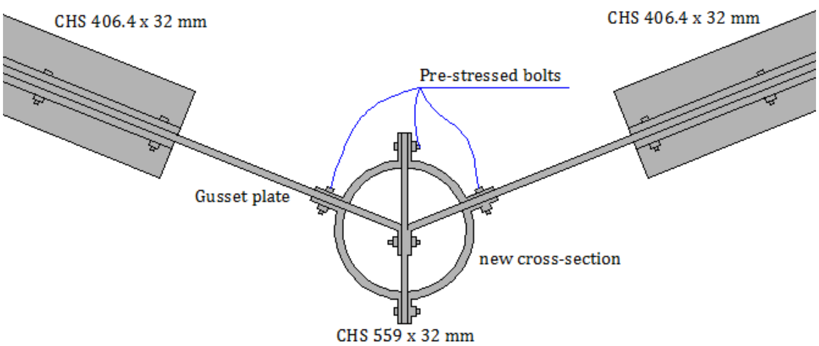

Figure 24: Top view of the connection.

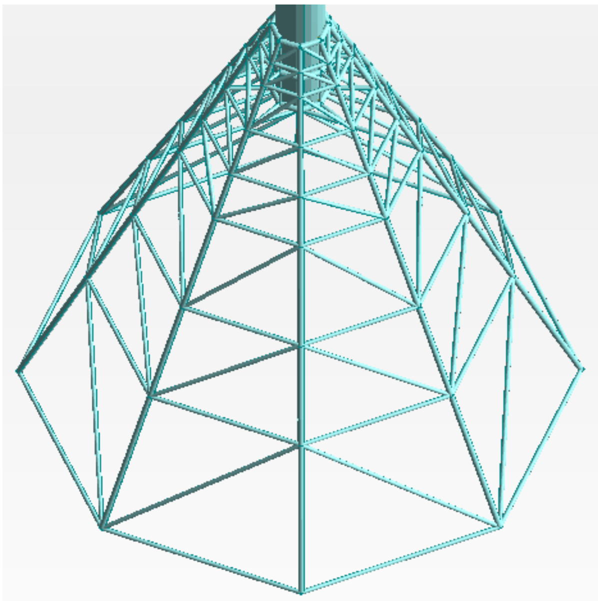

Figure 25: K-join on 3D view.

5.3 The Transition Element

Due to the high level of bending moment transmitted by the steel tubular tower, the element of transition is an important component of the tower. On this thesis suggests a conceptual element, which has a composition similar to others explained above. It is formed by two segments overlapped with 4560mm of high each one, composed of eight parts connected to each other by flanges, and between the flanges, a gusset plate is connected transmitting the efforts for the legs (see figure 26). As a gusset plate, the bending moments are neglected, only axial forces are considered on loads design. Is important to mention that, this work is only concerned with the design of the flanges of the transition piece and the gusset plate. The assessments are based on EC3-1-8 (CEN, 2005b), and a numerical analysis is performed (see Annex). Ductility criteria are ensured to avoid brittle failure and perform the plastic analysis.

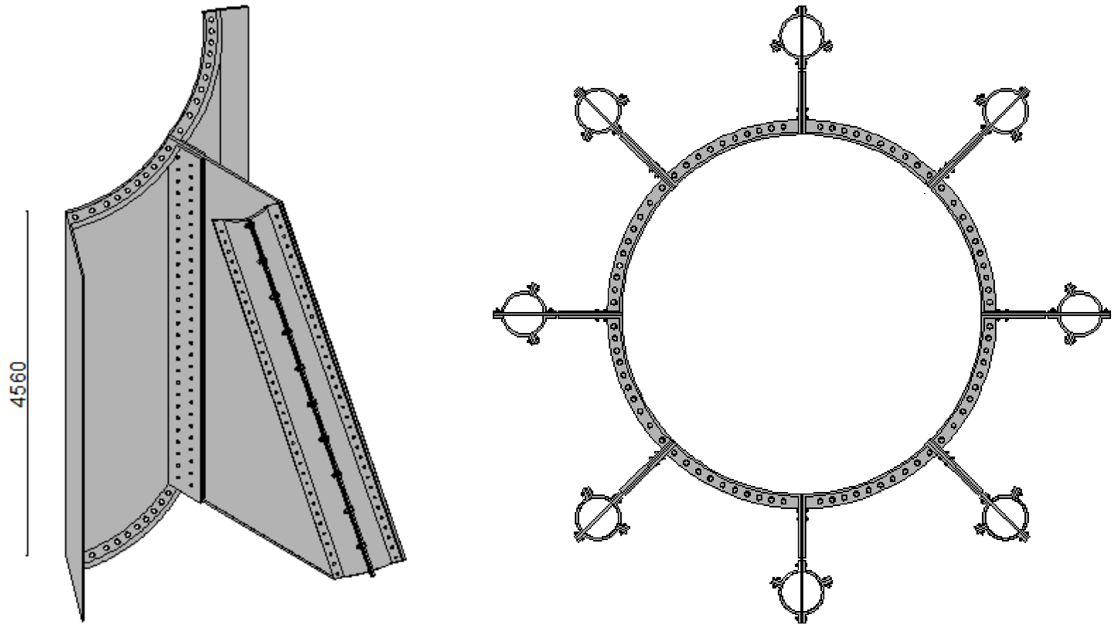

(a) (b)

Figure 26: a) 1/8 of one segment; b) Top view of transition piece.

Thickness of flange CHS 559 x 32 mm	10 mm
Thickness of gusset plate	30 mm
Thickness of flange transition element	20 mm
Numbers of pre-stressed bolts (M30) on CHS 559 x 32 mm	70 / segment
Numbers of pre-stressed bolts (M30) flange of transition p.	56 / segment

Table 20: Components of 1/8 transition element connections.

5.4 Numerical Analysis of K-Joint

A numerical analysis is performed for validations of results. The ductility requirements are considered avoiding the occurrence of brittle failures, especially in bolts, ensuring the plastic analysis. The partial safety factors γ_{Mi} for joints are given in table 21.

γ_{M0}	1.0
γ_{M1}	1.0
γ_{M2}	1.25
γ_{M3}	1.25
γ_{M7}	1.1

Table 21: Partial safety factors.

The design rules presented in this section are based on the resistance formule provided by EC 3-1-8 (CEN, 2005b), bolted joint section, at least as far as information is available. When this is not the case, the basic design principles prescribed by EC3-1-1 (CEN, 2005a) are followed. As mentioned on chapter 2, the steel class of gusset plate is S355 JR and the pre-stressed bolts are class 10.9. As shear connections, the pre-stressed bolts are classified as class C, which is established that slip should not occur at the ultimate limit state.

Category	Criteria	Remarks
C Slip-resistance at ultimate	$F_{v,Ed} \leq F_{s,Rd}$ $F_{v,Ed} \leq F_{b,Rd}$ $F_{v,Ed} \leq N_{net,Rd}$	Preloaded 8.8 or 10.9 bolts should be used.

Table 22: Categories of bolts connection – EC3-1-8, section 3.4 (CEN, 2005b).

Furthermore, is verified the resistance of others components of connections, as it can be seen on figure 27.

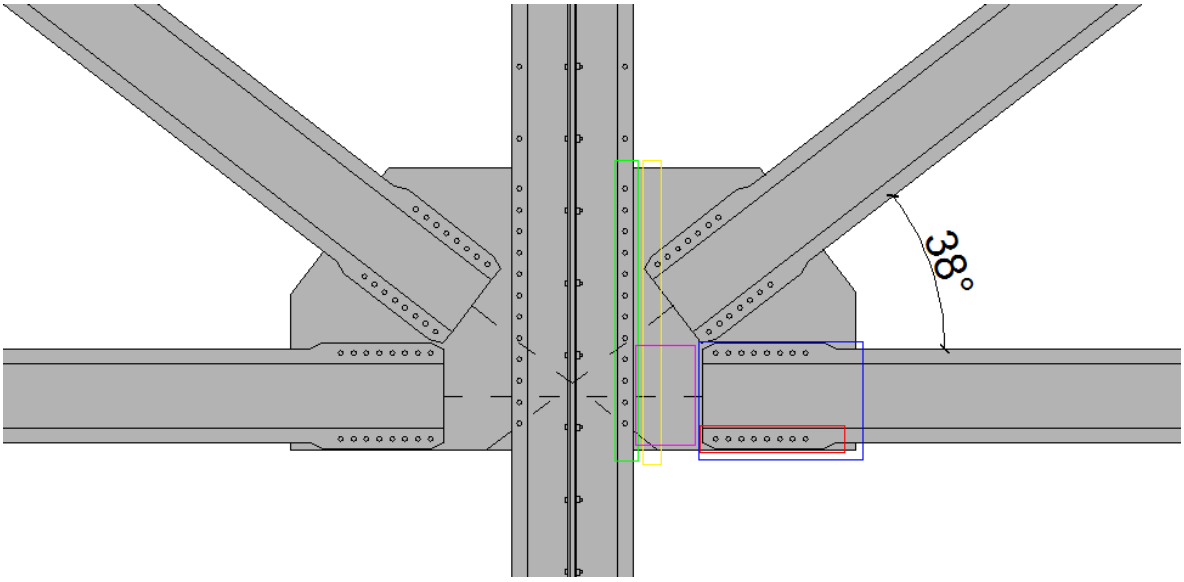

Figure 27: K-joint – Resistance verifications.

Where, is verified:

- Red rectangle: The resistance of the brace's flanges, due the fragility;
- Blue rectangle: The block tearing is verified, due the high tension forces;
- Yellow rectangle: The gross section resistance of the gusset plate, due the high level of tension force in both braces;
- Green rectangle: The share forces resistance of the components, due the vertical component of the braces;
- Cyan rectangle: The possibility of instability of gusset plate due the compression forces.

Classified as a pinned connection by EC3-1-8, section 5 (CEN, 2005b), which only transmit axial forces (see figure 12 and 13), the design loads are considered the extreme values, on ultimate limit states combinations, as demonstrate on figure 28.

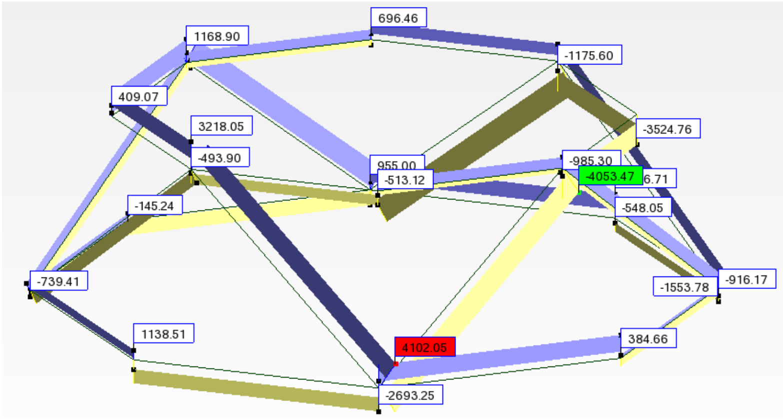

Figure 28: Diagram of axial forces – braces and horizontal braces form level 4.

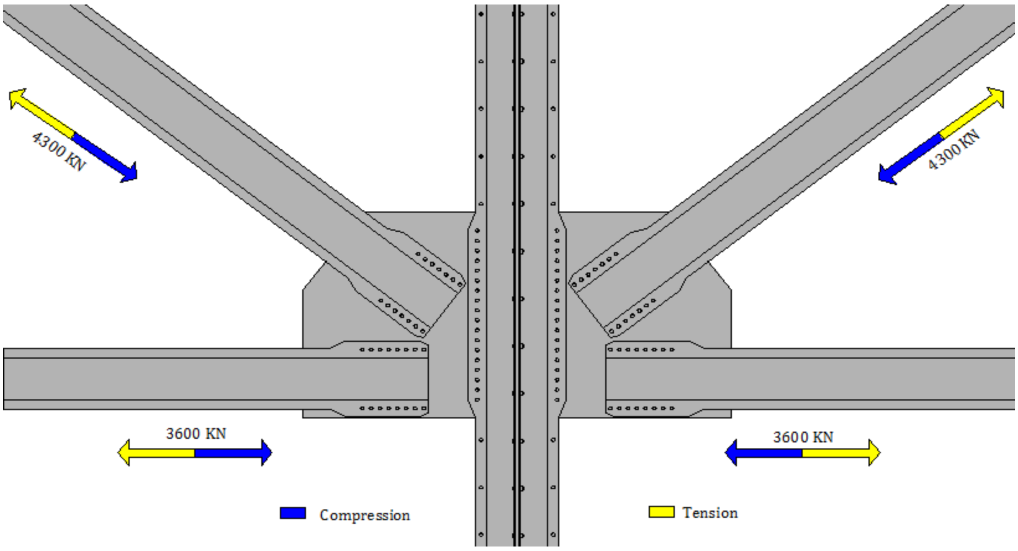

Figure 29: Extreme loads design (U.L.S).

The properties of bolts are showed on table 21 (for further information about the materials, see chapter 3).

fy (N/mm^2)	355.0
fu (N/mm^2)	430.0

Table 23: Steel properties.

Bolts	
Type	M30
A (mm^2)	561.0
Class	10.9
fu (N/mm^2)	1000.0
d (mm)	30.0
d_0 (mm)	33.0

Table 24: Bolts properties.

The position of holes of bolts and sizes are normalized according EC3-1-8, section 3.5 (CEN, 2005b).

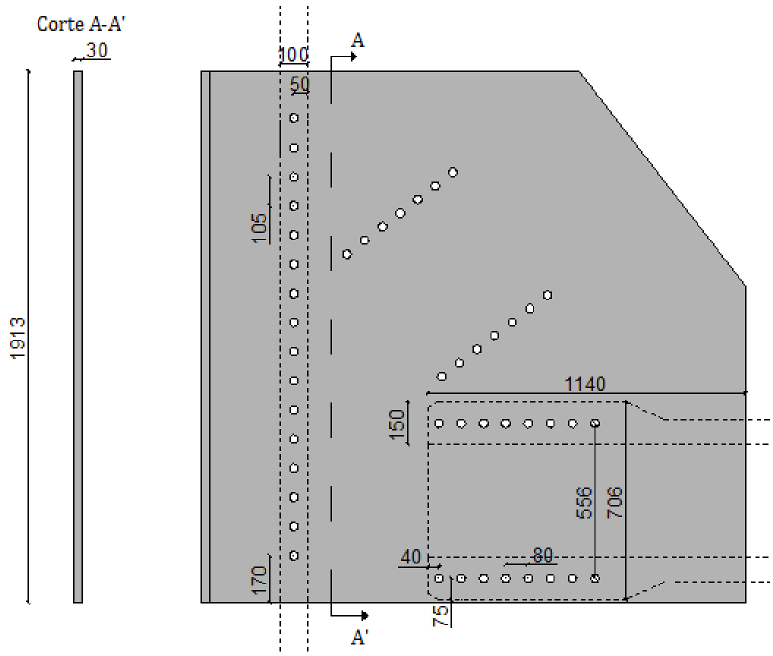

Figure 30: Position of holes and geometry of gusset plate (mm).

The first element to be studied is the connection of horizontal brace. The load design applied is N_{ed} = 3600.0 KN. As showed on figure 24, on this element are studied the fragility of flanges (red rectangle) and the block tearing (blue rectangle). The horizontal brace is composed by two parts of new cross-section; each part has two flanges, which are connected by the gusset plate, as demonstrated on figure 31 (or figure 24).

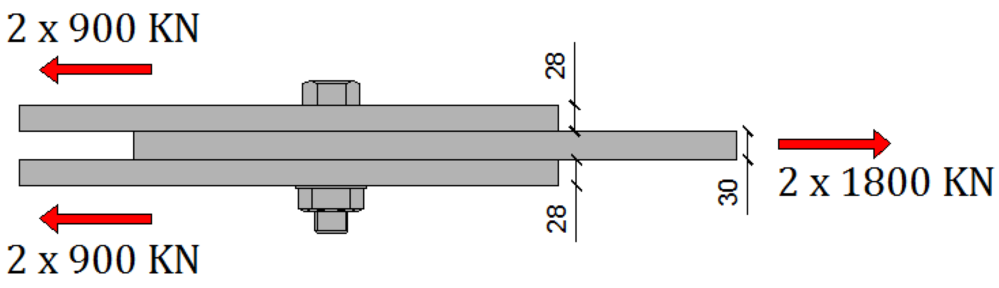

Figure 30: Outline of connection between flanges (of CHS 406.4 x 32mm) and gusset plate.

Spacing and edge distance (flange) – EC3-1-8, section 3.5	
e_1 (mm)	40.0
e_2 (mm)	75.0
p_1 (mm)	80.0

Table 25: Spacing and edge distance – flange CHS 406.4 x 32mm.

t_p (mm)	28.0
$h_{p,\ widht}$ (mm)	150.0
$h_{p,\ length}$ (mm)	1140.0

Table 26: Geometry properties of flange CHS 406.4 x 32mm (see figure 30).

The gusset plate is studied as a local component, when the studied is considered an element, like this point (a horizontal brace, see figure 30) , and a global component when it is considered two elements, which is studied on next point.

t_p (mm)	30.0
$h_{p\ widht}$ (mm)	706.0
$h_{p\ length}$ (mm)	1140.0

Table 27: Geometry properties of gusset plate local (CHS 406.4 x 32mm).

Spacing and edge distance (gusset plate) – EC3-1-8, section 3.5	
e_1 (mm)	80.0
e_2 (mm)	70.0
p_1 (mm)	80.0
p_2 (mm)	556.0

Table 28: Spacing and edge distance – gusset plate (CHS 406.4 x 32mm).

➢ Slip resistance (criteria $F_{v,Ed} \leq F_{s,Rd}$): EC3-1-8, section 3.9.1 (CEN, 2005b)

$$F_{p,Cd} = 0.7 \times f_{ub} \frac{A_s}{\gamma_{M7}} \qquad \text{(Eq. 5.4)}$$

$$F_{p,Cd} = 0.7 \times 1000.0 \times 10^3 \times \frac{561.0 \times 10^{-6}}{1.1} = 357.0 \text{ KN (design preloaded)}$$

$$F_{s,Rd} = \frac{K_s\, \eta\, \mu}{\gamma_{M3}} F_{P,c} \qquad \text{(Eq. 5.5)}$$

where, K_s is the coefficients for normal hole (K_s = 1.00);

η is the number of friction surface (see figure 24);

μ is the slip factor (μ = 0.50);

$$F_{s,Rd} = \frac{1.0 \times 2 \times 0.5}{1.25} \times 357.0 = 286.0 \text{ KN (one bolt)}$$

The slip resistance of one pre-stressed bolt is 286.00 KN; exist sixteen pre-stressed bolts linking the flanges with gusset plate (n = 16 pre-stressed bolts).

$$F_{s,Rd\ total} = 286.0 \times 16 = 4576.0 \text{ KN}$$

$$F_{V,Ed} = 3600.0 \text{ KN} \leq F_{s,Rd} = 4576.0 \text{ KN OK!!}$$

➢ Bearing resistance (criteria $F_{v,Ed} \leq F_{b,Rd}$): EC3-1-8, table 3.4 (CEN, 2005b); in this verification, the component which is studied is the flange (red rectangle, figure 27).

$$F_{b,Rd} = \frac{k_1\, \alpha_b\, f_u\, d\, t}{\gamma_{M2}} \qquad \text{(Eq. 5.6)}$$

where, $\alpha_b = \min.(\alpha_d; \frac{f_{ub}}{f_u}; 1.0)$

$$\alpha_b = \min.\left(0.4; \frac{1000}{490} = 2.0; 1.0\right) = 0.4$$

in the direction of load transfer:

for end bolts $\alpha_d = \frac{e_1}{3d_0}$; for inner bolts $\alpha_d = \frac{p_1}{3d_0} - \frac{1}{4}$:

$$\alpha_d = \frac{40.0}{3 \times 33.0} = 0.4; \qquad \alpha_d = \frac{80.0}{3 \times 33.0} - \frac{1}{4} = 0.6$$

perpendicular to the direction of load transfer:

- for edge bolts:

$$k_1 = \text{minimum}\left(2.8\frac{e_2}{d_0} - 1.7;\ 2.5\right) = \min.\left(2.8 \times \frac{75.0}{33.0} - 1.70 = 4.7; 2.5\right) = 2.5$$

- for inner bolts:

$$k_1 = minimum\left(1.4\,\frac{p_2}{d_0} - 1.7;\ 2.5\right) = \min.\left(1.4 \times \frac{0}{33.0} - 1.7 = 0;\ 2.5\right) = 2.5$$

$$F_{b,Rd} = \frac{2.5 \times 0.4 \times 490.0 * 10^3 \times 30.0 \times 10^{-3} \times 28.0 \times 10^{-3}}{1.25} = \frac{412.0}{1.25} = 329.0\ \text{KN}$$

The bearing resistance of one pre-stressed bolt is 329.0 KN; exist eight pre-stressed bolts linking each flange (n = 8 pre-stressed bolts).

$$F_{b,Rd\ total} = 329.0 \times 8 = 2634.2\ KN$$

$$F_{V,Ed} = 900.0\ KN \leq F_{b,Rd} = 2634.2\ KN\ \ OK!!$$

➢ Resistance of net cross-section of flange (criteria $F_{v,Ed} \leq N_{net,Rd}$) : EC3-1-1, section 6 (CEN, 2005b);

$$N_{net,Rd} = \frac{A_{net}\, f_y}{\gamma_{M0}} \tag{Eq.5.7}$$

$$A_{net} = h_p * t_p - n \times d_0 \times t_p = 150.0 \times 28.0 - 1 \times 33.0 \times 28.0 = 3276.0\ mm^2$$

n = 1 (number of bolt)

$$N_{net,Rd} = \frac{3276.0 \times 10^{-6} \times 355.0 \times 10^3}{1.0} = 1163.0\ KN$$

$$F_{V,Ed} = 900.0\ KN \leq N_{net,Rd} = 1163.0\ KN\ \ OK!!$$

So far, the verifications are dedicated for the flanges, due its fragility. Next, is verified the block tearing (blue rectangle, figure 27), where are studied both components, flange and plate.

➢ Block tearing (flange): EC3-1-8, section 3.10 (CEN, 2005b)

$$V_{eff,1,Rd} = \frac{f_u\, A_{nt}}{\gamma_{M2}} + \frac{\frac{1}{\sqrt{3}}\, f_y\, A_{nv}}{\gamma_{M0}} \tag{Eq. 5.8}$$

$$A_{nt} = t_p\left(e_2 - \frac{d_0}{2}\right)$$

$$A_{nt} = 28.0\left(75.0 - \frac{33.0}{2}\right) = 1638.0\ mm^2$$

$$A_{nv} = t_p\left(h_p - e_1 - (n_1 - 0.5) \times d_0\right)$$

$$A_{nv} = 28.0 \times (1140.0 - 40.0 - (8.0 - 0.5) \times 33.0) = 23870.0\ \mathrm{mm}^2$$

$$n_1 = 8.0\ (\text{n}^{\circ}\ \text{of bolts})$$

$$V_{eff,1,Rd} = \frac{490 \times 10^3 \times 1638 \times 10^{-6}}{1.25} + \frac{\frac{1}{\sqrt{3}} \times 355 \times 10^3 \times 23870 \times 10^{-6}}{1.0} = 5534.5\ \mathrm{KN}$$

$$F_{V,Ed} = 900.0\ \mathrm{KN} \leq F_{V,eff,1} = 5534.5\ \mathrm{KN}\ \ \text{OK!!}$$

- Block tearing (plate): EC3-1-8, section 3.10 (CEN, 2005b)

$$A_{nt} = 30.0\left(75.0 - \frac{33.0}{2}\right) = 1755.0\ \mathrm{mm}^2$$

$$A_{nv} = 30.0(1140.0 - 40.0 - (16.0 - 0.5) \times 33.0) = 17655.0\ \mathrm{mm}^2$$

$$n_1 = 16.0\ (\text{number of bolts})$$

$$V_{eff,1,Rd} = \frac{490 \times 10^3 \times 1755 \times 10^{-6}}{1.25} + \frac{\frac{1}{\sqrt{3}} \times 355 \times 10^3 \times 17655 \times 10^{-6}}{1.0} = 4306.5\ \mathrm{KN}$$

$$F_{V,Ed} = 3600\ \mathrm{KN} \leq F_{V,eff,1} = 4306.5\ \mathrm{KN}\ \ \text{OK!!}$$

On this verification the ductility criteria, for plastic analysis is achieved, being the block tearing of the gusset plate the failure component, as demonstrate on table 29.

Failure mode	Resistance forces (KN)
Slip resistance (pre-stressed bolts)	4576.0
Bearing resistance (flange)	$3688.0 \times 4_{flanges} = 14752.0$
Net cross-section resistance (flange)	$1163.0 \times 4_{flanges} = 4652.0$
Block tearing (flange)	$5534.5 \times 4_{flanges} = 22138.0$
Block tearing (plate)	4306.5

Table 29: Failure modes of braces connections.

Next step is the verification of tension forces on acting on global plate, yellow rectangle (figure 27). Due the inclination of the braces on diagonal, the force applied on this element is divided on component vertical and other horizontal. The angle, from horizontal brace, is 38 degrees. The horizontal component plus the force applied on horizontal brace forming the design load.

$$N_{Ed} = \cos 38° \times 4300\ KN = 3389.0\ KN + 3600\ KN \cong 7000\ KN$$

$$N_{Ed} \leq N_{t,Rd} \quad \text{(Eq. 5.9)}$$

$$N_{pl,Rd} = \frac{A\, f_y}{\gamma_{M0}} = \frac{57390.0 \times 10^{-6} \times 355.0 \times 10^{3}}{1.0} = 20373.5\ KN \quad \text{(Eq. 5.10)}$$

$$A = 1913.0 \times 30.0 = 57390.0\ mm^2$$

$$N_{Ed} = 7000.0\ KN \leq N_{t,Rd} = 20373.5\ KN \ \text{ OK!!}$$

The vertical component of diagonal brace is applied as a shear force on the connection, green rectangle, being necessary verified that zone. The load applied is Ned = 2650.0 KN. All verifications are directed for the flange, which is component more fragile, less thickness than gusset plate.

Spacing and edge distance (flange) – EC3-1-8, section 3.5	
e_1 (mm)	170.0
e_2 (mm)	85.0
p_1 (mm)	94.0

Table 30: Spacing and edge distance – flange CHS 559 x 32mm.

t_p (mm)	10.0
$h_{p,\ horizontal}$ (mm)	100.0
$h_{p,\ vertical}$ (mm)	1941.0

Table 31: Geometry properties of flange CHS 559.0 x 32mm (see figure 30).

- Slip resistance (criteria $F_{v,Ed} \leq F_{s,Rd}$): EC3-1-8, section 3.9.1 (CEN, 2005b)

$$F_{p,Cd} = 0.7 \times 1000.0 \times 10^3 \times \frac{561.0 \times 10^{-6}}{1.1} = 357.0 \text{ KN (design preloaded)}$$

$$F_{s,Rd} = \frac{1.0 \times 2 \times 0.5}{1.25} \times 357.0 = 286.0 \text{ KN (one bolt)}$$

The slip resistance of one pre-stressed bolt is 286.00 KN; exist eighteen pre-stressed bolts linking the flanges with gusset plate (n = 18 pre-stressed bolts).

$$F_{s,Rd\ total} = 286.0 \times 18 = 5140.8 \text{ KN}$$

$$F_{V,Ed} = 2650.0 \text{ KN} \leq F_{s,Rd} = 5140.8 \text{ KN OK!!}$$

➢ Bearing resistance (criteria $F_{v,Ed} \leq F_{b,Rd}$): EC3-1-8, table 3.4 (CEN, 2005b); on this verification, the component which is studied is the flange (green rectangle, figure 27).

$$\alpha_b = \min.\left(0.7; \frac{1000}{490} = 2.0; 1.0\right) = 0.7$$

$$\alpha_d = \frac{170.0}{3 \times 33.0} = 1.7; \qquad \alpha_d = \frac{94}{3 \times 33.0} - \frac{1}{4} = 0.7$$

perpendicular to the direction of load transfer:

- for edge bolts:

$$k_1 = \text{minimum}\left(2.8\frac{e_2}{d_0} - 1.7;\ 2.5\right) = \min.\left(2.8 \times \frac{85.0}{33.0} - 1.70 = 5.51; 2.5\right) = 2.5$$

- for inner bolts:

$$k_1 = minimum\left(1.4\ \frac{p_2}{d_0} - 1.7;\ 2.5\right) = \min.\left(1.4 \times \frac{0}{33.0} - 1.7 = 0;\ 2.5\right) = 2.5$$

$$F_{b,Rd} = \frac{2.5 \times 0.7 \times 490.0 * 10^3 \times 30.0 \times 10^{-3} \times 10.0 \times 10^{-3}}{1.25} = \frac{257.0}{1.25} = 206.0 \text{ KN}$$

The bearing resistance of one pre-stressed bolt is 206.0 KN; exists eighteen pre-stressed bolts linking the flange with the gusset plate (n = 18 pre-stressed bolts).

$$F_{b,Rd\ total} = 206.0 \times 18 = 3708.0\ KN$$

$$F_{V,Ed} = \frac{2650.0}{2_{flanges}} = 1325.0\ KN \leq F_{b,Rd} = 3708.0\ KN\ \ OK!!$$

➢ Resistance of net cross-section of flange (criteria $F_{v,Ed} \leq N_{net,Rd}$) : EC3-1-1, section 6 (CEN, 2005b);

$$V_{Rd} = \frac{A_{v,net}}{\sqrt{3}} \frac{f_u}{\gamma_{M2}} \qquad \text{(Eq. 5.11)}$$

$$A_{v,net} = h_p * t_p - n \times d_0 \times t_p = 1941.0 \times 10.0 - 18.0 \times 33.0 \times 10.0 = 13470.0\ mm^2$$

n = 18 (number of bolt)

$$V_{net,Rd} = \frac{13470.0 \times 10^{-6}}{\sqrt{3}} \frac{490.0 \times 10^3}{1.25} = 3048.6\ KN$$

$$F_{V,Ed} = \frac{2650.0}{2_{\ flanges}} = 1325.0\ KN \leq V_{net,Rd} = 3048.6\ KN\ \ OK!!$$

➢ Block tearing (flange): EC3-1-8, section 3.10 (CEN, 2005b)

$$V_{eff,2,Rd} = 0.5 \frac{f_u A_{nt}}{\gamma_{M2}} + \frac{\frac{1}{\sqrt{3}} f_y A_{nv}}{\gamma_{M0}} \qquad \text{(Eq. 5.12)}$$

$$A_{nt} = 10.0\left(85.0 - \frac{33.0}{2}\right) = 685.0\ mm^2$$

$$A_{nv} = 10.0 \times (1941.0 - 170.0 - (18.0 - 0.5) \times 33.0) = 11937.0 mm^2$$

$n_1 = 18.0$ (n^o of bolts)

$$V_{eff,2,Rd} = 0.5 \times \frac{490 \times 10^3 \times 685 \times 10^{-6}}{1.25} + \frac{\frac{1}{\sqrt{3}} \times 355 \times 10^3 \times 11937 \times 10^{-6}}{1.0} = 2480\ KN$$

$$F_{V,Ed} = \frac{2650}{2_{flanges}} = 1325.0\ KN \leq F_{V,eff,1} = 2480.0\ KN\ \ OK!!$$

Failure mode	Resistance forces (KN)
Slip resistance (pre-stressed bolts)	5140.8
Bearing resistance (flange)	$3708.0 \times 2_{flanges} = 7416.0$
Net cross-section resistance (flange)	$3048.6 \times 2_{flanges} = 6097.2$
Block tearing (flange)	$2480.0 \times 2_{flanges} = 4960.0$

Table 32: Failure mode of legs connection.

The cyan rectangle represents the area of gusset plate that is on compression. The verification of instability is provided according EC3-1-1. It's considered that, the diffusion of compression forces makes an angle from the horizontal line equal zero, as demonstrated on figure 32. To determine the buckling length, it is considered both sides of the element pined, $L_E = L$.

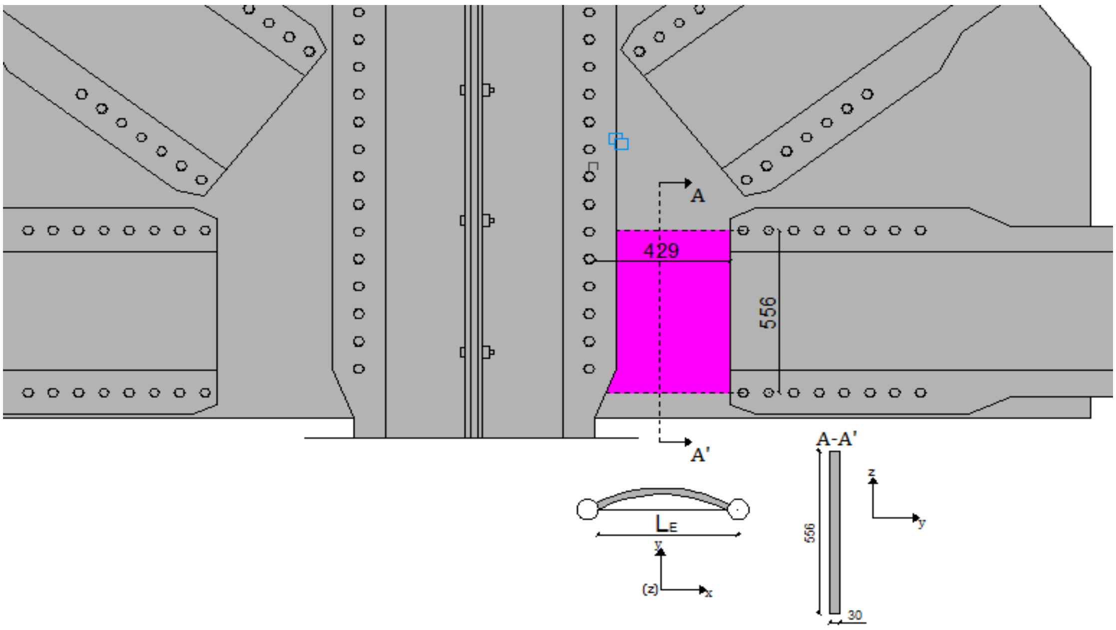

Figure 31: Compression area and buckling length (mm).

A (mm^2)	16700.0
I_y (mm^4)	429700000.0
I_z (mm^4)	1251000.0
b (mm)	30.0
h (mm)	556.0
i_y (mm)	161.0
i_z (mm)	9.0

Table 33: Geometry properties (A –A').

➢ Resistance of cross-section A-A': EC3-1-1, section 6.2 (CEN, 2005a).

$$\frac{N_{Ed}}{N_{c,Rd}} \leq 1.0 \quad \text{(Eq. 5.13)}$$

$$N_{c,Rd} = \frac{A\, f_y}{\gamma_{M0}} = \frac{16700 \times 10^{-6} \times 355 \times 10^3}{1.0} = 5928.5\ \text{KN} \quad \text{(Eq. 5.14)}$$

$$\frac{3600.0}{5928.5} \cong 0.6 \leq 1.0\ \text{OK!!}$$

➢ Buckling resistance of members:

$$\frac{N_{Ed}}{N_{b,Rd}} \leq 1.0 \quad \text{(Eq. 5.15)}$$

$$N_{b,Rd} = \frac{\chi\, A\, f_y}{\gamma_{M1}} \quad \text{(Eq. 5.16)}$$

Plane x-z:

L_{Ey} = 432.0mm

Plane x-y:

L_{Ez} = 432.0mm

$$\lambda_1 = \pi\sqrt{\frac{210 \times 10^6}{355 \times 10^3}} = 70.4$$

$$\lambda_y = \frac{L_{Ey}}{i_y} = \frac{432.0}{161.0} = 2.68; \qquad \bar{\lambda}_y = \frac{\lambda_y}{\lambda_1} = \frac{2.68}{70.4} = 0.04$$

$$\lambda_z = \frac{L_{Ez}}{i_z} = \frac{432.0}{9} = 48.0; \qquad \bar{\lambda}_z = \frac{\lambda_z}{\lambda_1} = \frac{48.0}{70.4} = 0.68$$

$$\frac{h}{b} = \frac{556.0}{30} = 18.5 > 1.2;$$

$$\text{Buckling about axis: } y - y = \text{curve a} = 0.21;\ \ z - z = \text{curve b} = 0.34;$$

$$\bar{\lambda}_z > \bar{\lambda}_y \text{ and } \alpha_{\text{curve b}} > \alpha_{\text{curve a}} => \chi_{min} = \chi_z$$

$$\emptyset = 0.5[1 + \alpha(\bar{\lambda} - 0.2) + \bar{\lambda}^2 = 0.5[1 + 0.34 \times (0.68 - 0.2) + 0.68^2 = 0.81$$

$$\chi_z = \frac{1}{0.81 + \sqrt{0.81^2 - 0.68^2}} = 0.80$$

$$N_{b,Rd} = \frac{0.8 \times 16700.0 \times 10^{-6} \times 355.0 \times 10^3}{1.0} = 4742.8 \text{ KN OK!!}$$

$$\frac{3600.0}{4742.8} = 0.76 \leq 1.0 \text{ OK!!}$$

On figure 26 is represented the connection on bottom of the tower, where the braces are madden 38^o with the horizontal braces, which cause an eccentricity of 80mm. On others connections on tower, the angle increases and the eccentricity is zero.

According EC3-1-8, section 5 (CEN, 2005b), the moments resulting by eccentricities may be neglected in the design if the eccentricities are within the following limit:

$$-0.55 \times d_0 \leq e \leq 0.25 \times d_0 = -0.55 \times 33 \leq 80 \leq 0.25 \times 559 = -18.2 \leq 80 \leq 140 \text{ OK!}$$

where, e is the eccentricity defined on figure 27

d_0 is the diameter of the chord

After all connection verifications of the lattice tower, it can be concluding that connections are a rigid component of the tower. To avoiding brittle failure, through the bolts, was verified all components to ensure the ductile requirements and fulfill all standards on EC3 (CEN, 2005b).

Components	
Thickness of flanges (CHS 406.4 x 32 mm)	28 mm
Thickness of flanges (CHS 559 x 32 mm)	10 mm
Gusset plate	30 mm
Pre-stressed bolts	M30

Table 34: Properties of connection components.

5.5 Fatigue Limit State

Fatigue failure takes place by the initiation and propagation of a crack until the crack becomes unstable and propagates fast, if not suddenly, to failure. To ensure that a structure will fulfill its intended function, fatigue assessment, supported where appropriate by a detailed fatigue analysis, should be carried out for each type of structural detail, which is subjected to extensive dynamic loading (DNV/RIso, 2002). On this case of study, the assessment of fatigue limit state is performed on connections, due the fragility of its components susceptible to failure. The fatigue design is based S-N curves present on EC3-1-9 (CEN, 2005c), section 7, which correspond to typical detail categories that are designated by a number which represents, in N/mm^2, the reference value $\Delta\sigma_C$ and $\Delta\tau_C$ for the fatigue strength at 2 million cycles, with the slope of fatigue strength curve, m=3 and $N_{ref} = 2.0 \times 10^8$.

$$\Delta\sigma_R^m \times N_{ref} = \Delta\sigma_c^m \times 2 \times 10^6 \qquad \text{(Eq. 5.17)}$$

$$\Delta\sigma_c^3 = \Delta\sigma_R^3 \times \frac{2 \times 10^8}{2 \times 10^6}$$

$$\Delta\sigma_c = \Delta\sigma_R \times \left(\frac{2 \times 10^8}{2 \times 10^6}\right)^{\frac{1}{3}} => \Delta\sigma_c = \Delta\sigma_R \times \sqrt[3]{100} \quad \text{(Eq. 5.18)}$$

On figure 33, is demonstrated the way of forces to comprehend the sections considered for study. As explained previously, the design loads considered are axial forces, thus the damage equivalent load deemed are ΔF_x = 203 KN. The study is basically calculating the yield stress on section A – A' and B – B', determine the reference value according the equation 5.18, and compare with the reference value that is obtained on EC3-1-9, section 7 (CEN, 2005c). On this case, double covered symmetrical joint with preloaded high strength bolts, the reference value to be compared is $\Delta\sigma_c$ = 112 MPa.

The section A – A' is composed by two flanges with 28mm of thickness and the plate with 30mm. On section B – B', the thickness of flanges and plate are 10mm and 30mm respectively.

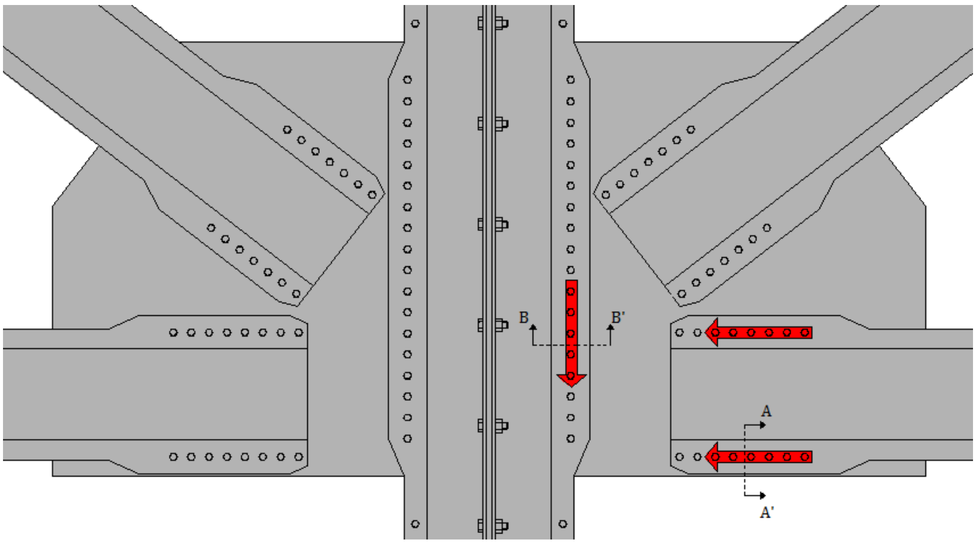

Figure 32: Way of axial load and sections A – A' and B – B',

Section A – A':

$$\Delta F_x = \frac{203.0}{2_{ways}} = 101.5 \text{ KN}$$

$$\text{Area} = (150.0 \times (28.0 + 30.0 + 28.0)) = 12900.0 \text{ mm}^2$$

$$\Delta\sigma_R = \frac{101.5}{12900.0 \times 10^{-6}} = 7868.2 \text{ KPa} \times 10^{-3} \cong 7.9 \text{ MPa}$$

$$\Delta\sigma_c = \Delta\sigma_R \times \sqrt[3]{100} = 36.7 \text{ MPa} < 112.0\ MPa\ OK!!$$

<u>Section B – B:</u>

$\Delta F_x = 203.0$ KN

Area $= (170 \times (10 + 30 + 10)) = 8500.0 \text{ mm}^2$

$$\Delta\sigma_R = \frac{203.0}{8500.0 \times 10^{-6}} = 23882.0 \text{ KPa} \times 10^{-3} \cong 23.9 \text{ MPa}$$

$$\Delta\sigma_c = 23.9 \times \sqrt[3]{100} = 110.9\text{MPa} < 112.0\ MPa\ OK!!$$

On transition element, the fatigue is verified on link among flanges of CHS 559 x 32mm element and gusset plate, gusset plate and flanges of transition piece. The sections C – C' is composed by 10mm / 30mm / 10mm of thickness and the section D – D' by 20mm / 30mm / 20mm of thickness.

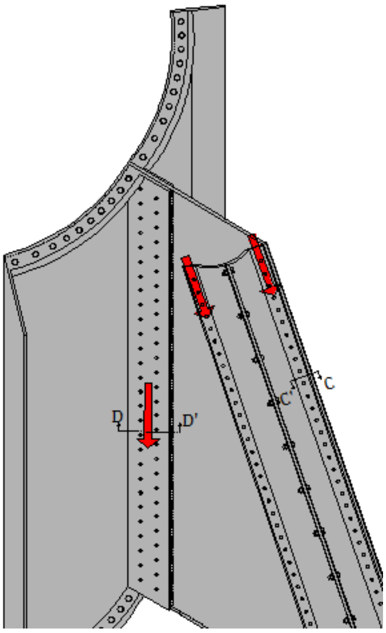

Figure 33: The way of forces on transition piece

Section C – C’:

$$\Delta F_x = \frac{203.0}{2_{ways}} = 101.5 \text{ KN}$$

$$\text{Area} = \left(150.0 \times (10.0 + 30.0 + 10.0)\right) = 7500.0 \text{ mm}^2$$

$$\Delta\sigma_R = \frac{101.5}{7500.0 \times 10^{-6}} = 13533.3 \text{ KPa} \times 10^{-3} \cong 13.5 \text{ MPa}$$

$$\Delta\sigma_c = \Delta\sigma_R \times \sqrt[3]{100} = 62.8 \text{ MPa} < 112.0\ MPa\ \ OK!!$$

Section D – D’:

$$\Delta F_x = 203.0 \text{ KN}$$

$$\text{Area} = \left(520.0 \times (20.0 + 30.0 + 20.0)\right) = 36400.0 \text{ mm}^2$$

$$\Delta\sigma_R = \frac{203.0}{36400 \times 10^{-6}} = 5577.0 \text{ KPa} \times 10^{-3} \cong 5.6 \text{ MPa}$$

$$\Delta\sigma_c = \Delta\sigma_R \times \sqrt[3]{100} = 25.9 \text{ MPa} < 112.0 \text{ MPa OK!!}$$

After the validation of the results, it can be conclude that the fatigue limit state influence the geometry of the connection, increasing the width of the flange connections avoiding the fatigue failure, as shown on figure 33.

6 CONCLUSIONS

With the increasing of the market share of wind power on renewable energy industry, new solutions of wind towers and new technologies appear due to the tendency of increasing the height, and also to become greater efficient energetically. High hub over 120m becomes issue of transportation and high cost of manufacturing. So that, conceptual hybrid lattice-tubular steel onshore wind tower was proposed.

As explained before in chapter 4, the lattice tower is a rigid structure capable to tolerate the efforts transmitted by the steel tubular tower. Verifications on the stability and resistance of three elements of the tower were made, such as an element with more bending on the top, a slender element on bottom of the tower, and a compression element on bottom of the tower. The results have shown that the stiffness of the tower is influenced by a global analysis, decreasing the ratio of local optimization process, as demonstrated in table 18.

The use of new cross-sections on elements of the lattice tower and on the conceptual transition piece will accelerate the process of assemble and facility of the transportation. The efficient link between the gusset plate with the braces and legs allow a rigid connection, as demonstrated in chapter 5. Those geometry properties are influenced by the fatigue limit state.

In order to quantify the advantages of the hybrid solution, a comparative study of self-weight and quantities of concrete used on foundation, between a 150m of steel tubular tower and the hybrid lattice tubular steel tower was made. A pad foundation was used as a pinned solution on the support of superstructure to avoid the transmission of bending moments. The comparative values of 150 meters of steel tubular tower are obtained from (Carlos Rebelo, 2013). A quick design process of the pad foundation is based on the punching share requirements established on EC2-1-1 (CEN, 2004a). The design process is presented on Annex B.

Ø' k	42°
c'k (KPa)	0
γ (KN/m³)	18.0
E (MPa)	675.0

Table 35: Soil properties considered.

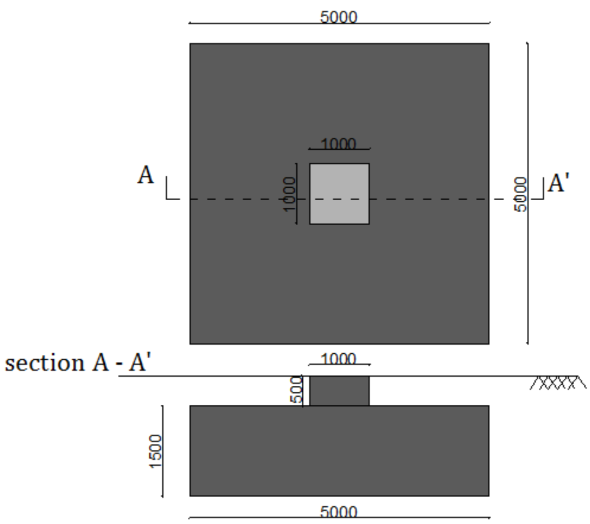

Figure 34: Pad foundation of lattice tower considered.

$$\text{Volume}_{\text{concrete}} = 5.0 \times 5.0 \times 1.5 + 0.5 \times 1.0 \times 1.0 = 38.0\text{m}^3 \text{ (one leg foundation)}$$

$$\text{Volume}_{\text{total}} = 38.0 \times 8_{\text{legs}} = 304.0\text{m}^3$$

Based on (Carlos Rebelo, 2013), the foundation quantity of concrete and self-weight of steel structure of a 150m steel tubular wind tower is 981.9m^3 and 1025 tons respectively. In this work, according to an expedite foundation design, the quantity of concrete used in foundations is approximately 300m^3, and the self-weight of the proposed hybrid solution is about 1015 tons.

Thus, it can be concluded that the amount of steel used in the hybrid wind tower is similar to the one used in tubular tower. The most important advantages of the proposed solution are the transportation, the assembly readiness and the considerable reduction of the foundations.

Self-weight $_{\text{lattice tower}}$ (tons)	$665.4 \times 5\%_{connections} = 699.0$
Self-weight $_{\text{global structure}}$ (tons)	1015.0
Concrete $_{\text{foundation}}$ (m^3)	304.0

Table 36: Characteristics of hybrid lattice-tubular steel wind tower

REFERENCES

Rebelo, C., Veljkovic, M., Matos, R., & da Silva, L. S. (2012). Structural monitoring of a wind turbine steel tower – Part II: monitoring results. Wind and Structures, Vol. 15 (4).

Veljkovic, M., Feldmann, M., Naumes, J., Pak, D., Rebelo, C., & da Silva, L. S. (2010). Friction connection in tubular towers. Stahlbau, 660-668.

Veljkovic, M., Feldmann, M., Naumes, J., Pak, D., da Silva, L. S., & Rebelo, C. (2010). Wind turbine tower design, erection and maintenance. Woodhead Publishing Limited, 276-304.

Rebelo C., Moura, A., Gervásio H., Veljkovic M., Simões da Silva, L. (2013). Comparative Life Cycle Assessment Of Tubular Wind Towers And Foundations - Part 1: Structural Design (submitted for publication).

DNV/RIso. (2002). Guidelines of Design of Wind turbines (Second edition ed.). Denmark.

Elforsk . (2012, January). Cracks in onshore wind power - Causes and consequences. Elforsk rapport 11:56.

EWEA - The European Wind Energy Association. (February 2012). Wind in power - 2011 European statistics. Belgium.

GWEC - Global Wind Energy Council. (2012). GWEC - Global Wind Energy Council. Obtido de http://www.gwec.net

Hau, E. (2006). Wind turbines - Fundamentals, Technologies, Application, Economics (2nd ed.). Germany: Springer.

Providência, P. (2008). Sebenta de Teoria das estruturas I. Portugal.

Rebelo, C. (2012). Design Loads to be considered for tower and foundation design. Coimbra.

Rebelo, C., Veljkovic, M., da Silva, L. S., Simões, R., & Henriques, J. (2012). Structural monitoring of a wind turbine steel - Part I: system description and calibration. Wind and Structures, Vol. 15 (4).

Simões, R. A. (2007). Manual de dimensionamento de estruturas metálicas (segunda edição ed.). Portugal: CMM - Associação portuguesa de construção metálica mista.

UN-Energy. (2013, Abril 8). UN-Energy - knowledge network. Retrieved from http://www.unenergy.org/

Vattenfall. (2011). Towards sustainable energy - Corporate Social Renponsibility. Sweden.

CEN (2001) 1990-1-1: 2001, "Eurocode - Basis of structural design", European Committee for Standardization, 2010.

CEN (2002a) 1991-1-1: 2002, "Eurocode 1 - Actions on structures - Part 1-1: General actions - Densities, self-weight, imposed loads for buildings", European Committee for Standardization, Brussels.

CEN (2004a) 1992-1-1: 2004, "Eurocode 2 - Design of concrete structure - Part 1-1: General rules and rules for buildings", European Committee for Standardization, Brussels.

CEN (2005a) 1993-1-1: 2005, "Eurocode 3 - Design of steel structures - Part 1-1: General rules and rules for buildings", European Committee for Standardization, Brussels.

CEN (2005b) 1993-1-8:2005, "Eurocode 3 - Design of steel structures - Part 1-8: Design of joints ", European Committee for Standardization, Brussels.

CEN (2005c) 1993-1-9:2005, "Eurocode 3 - Design of steel structure - Part 1-9: Fatigue", European Committee for standardization, Brussels.

CEN (2004b) 10025-2:2004, "Hot rolled products of structural steels. Technical delivery conditions for non-alloy structural steels", European Committee for Standardization, Brussels.

CEN (1994) 10210-1:1994, " Hot finished structural hollow sections of non-alloy and fine grain structural steels - Part 1: Technical delivery requirements", European Committee for Standardization, Brussels.

CEN (2002b) 14399:2002, Group 4 " High strength structural bolting for preloading", European Committee for Standardization, Brussels.

CEN (2008) 1090-2:2008, Group 7 " Execution of steel structures and aluminium structures - Part 2: Technical requirements for steel structures", European Committee for Standardization, Brussels.

ANNEX

ANNEX A.1

Connection of diagonal brace CHS 406.4 x 32mm:

N_{ed} = 4300.0 KN

Spacing and edge distance (flange) – EC3-1-8, section 3.5	
e_1 (mm)	40.0
e_2 (mm)	75.0
p_1 (mm)	80.0

Table 37: Spacing and edge distance – flange CHS 406.4 x 32mm.

t_p (mm)	28.0
$h_{p,\ widht}$ (mm)	150.0
$h_{p,\ length}$(mm)	1140.0

Table 38: Geometry properties of flange CHS 406.4 x 32mm (see figure 29).

The gusset plate is studied as a local component, when on the studied is considered an element (a horizontal brace, see figure 29), like this point, and a global component when it is considered two elements, which is studied on next point.

t_p (mm)	30.0
$h_{p\ widht}$ (mm)	706.0
$h_{p\ length}$ (mm)	1140.0

Table 39: Geometry properties of gusset plate local (CHS 406.4 x 32mm).

Spacing and edge distance (gusset plate) – EC3-1-8, section 3.5	
e_1 (mm)	80.0
e_2 (mm)	70.0
p_1 (mm)	80.0
p_2 (mm)	556.0

Table 40: Spacing and edge distance – gusset plate (CHS 406.4 x 32mm).

- Slip resistance (criteria $F_{v,Ed} \leq F_{s,Rd}$): EC3-1-8, section 3.9.1 (CEN, 2005b)

$$F_{p,Cd} = 0.7 \times 1000.0 \times 10^3 \times \frac{561.0 \times 10^{-6}}{1.1} = 357.0 \text{ KN (design preloaded)}$$

$$F_{s,Rd} = \frac{K_s\ \eta\ \mu}{\gamma_{M3}} F_{P,c}$$

where, K_s is the coefficients for normal hole (K_s = 1.00);

η is the number of friction surface (see figure 24);

μ is the slip factor (μ = 0.50);

$$F_{s,Rd} = \frac{1.0 \times 2 \times 0.5}{1.25} \times 357.0 = 286.0 \text{ KN (one bolt)}$$

The slip resistance of one pre-stressed bolt is 286.00 KN; exist sixteen pre-stressed bolts linking the flanges with gusset plate (n = 16 pre-stressed bolts).

$$F_{s,Rd\ total} = 286.0 \times 16 = 4576.0 \text{ KN}$$

$$F_{V,Ed} = 3600.0 \text{ KN} \leq F_{s,Rd} = 4576.0 \text{ KN OK!!}$$

- Bearing resistance (criteria $F_{v,Ed} \leq F_{b,Rd}$): EC3-1-8, table 3.4 (CEN, 2005b); on this verification, the component which is studied is the flange (red rectangle, figure 24).

$$F_{b,Rd} = \frac{k_1\, \alpha_b\, f_u\, d\, t}{\gamma_{M2}}$$

where, $\alpha_b = \min.(\alpha_d; \frac{f_{ub}}{f_u}; 1.0)$

$$\alpha_b = \min.\left(0.4; \frac{1000}{490} = 2.0; 1.0\right) = 0.4$$

in the direction of load transfer:

for end bolts $\alpha_d = \frac{e_1}{3d_0}$; for inner bolts $\alpha_d = \frac{p_1}{3d_0} - \frac{1}{4}$:

$$\alpha_d = \frac{40.0}{3 \times 33.0} = 0.4; \qquad \alpha_d = \frac{80.0}{3 \times 33.0} - \frac{1}{4} = 0.6$$

perpendicular to the direction of load transfer:

- for edge bolts:

$$k_1 = \text{minimum}\left(2.8\frac{e_2}{d_0} - 1.7;\ 2.5\right) = \min.\left(2.8 \times \frac{75.0}{33.0} - 1.70 = 4.7; 2.5\right) = 2.5$$

- for inner bolts:

$$k_1 = minimum\left(1.4\,\frac{p_2}{d_0} - 1.7;\ 2.5\right) = \min.\left(1.4 \times \frac{0}{33.0} - 1.7 = 0;\ 2.5\right) = 2.5$$

$$F_{b,Rd} = \frac{2.5 \times 0.4 \times 490.0 * 10^3 \times 30.0 \times 10^{-3} \times 28.0 \times 10^{-3}}{1.25} = \frac{412.0}{1.25} = 329.0\ \text{KN}$$

The bearing resistance of one pre-stressed bolt is 329.0 KN; exist eight pre-stressed bolts linking each flange (n = 8 pre-stressed bolts).

$$F_{b,Rd\ total} = 329.0 \times 8 = 2634.2\ \text{KN}$$

$$F_{V,Ed} = 900.0\ \text{KN} \leq F_{b,Rd} = 2634.2\ \text{KN OK!!}$$

➢ Resistance of net cross-section of flange (criteria $F_{v,Ed} \leq N_{net,Rd}$) : EC3-1-1, section 6 (CEN, 2005b);

$$N_{net,Rd} = \frac{A_{net}\, f_y}{\gamma_{M0}}$$

$$A_{net} = h_p * t_p - n \times d_0 \times t_p = 150.0 \times 28.0 - 1 \times 33.0 \times 28.0 = 3276.0\ mm^2$$

n = 1 (number of bolt)

$$N_{net,Rd} = \frac{3276.0 \times 10^{-6} \times 355.0 \times 10^3}{1.0} = 1163.0\ KN$$

$$F_{V,Ed} = 900.0\ KN \leq N_{net,Rd} = 1163.0\ KN \ \text{ OK!!}$$

So far, the verifications are dedicated for the flanges, due its fragility. Next, the block tearing is verified, where both components flange and plate are studied.

➢ Block tearing (flange): EC3-1-8, section 3.10 (CEN, 2005b)

$$V_{eff,1,Rd} = \frac{f_u\, A_{nt}}{\gamma_{M2}} + \frac{\frac{1}{\sqrt{3}}\, f_y\, A_{nv}}{\gamma_{M0}}$$

$$A_{nt} = t_p\left(e_2 - \frac{d_0}{2}\right)$$

$$A_{nt} = 28.0\left(75.0 - \frac{33.0}{2}\right) = 1638.0\ mm^2$$

$$A_{nv} = t_p\left(h_p - e_1 - (n_1 - 0.5) \times d_0\right)$$

$$A_{nv} = 28.0 \times (1140.0 - 40.0 - (8.0 - 0.5) \times 33.0) = 23870.0\ mm^2$$

$n_1 = 8.0$ (n° of bolts)

$$V_{\mathrm{eff,1,Rd}} = \frac{490 \times 10^3 \times 1638 \times 10^{-6}}{1.25} + \frac{\frac{1}{\sqrt{3}} \times 355 \times 10^3 \times 23870 \times 10^{-6}}{1.0} = 5534.5 \text{ KN}$$

$$F_{\mathrm{V,Ed}} = 900.0 \text{ KN} \leq F_{\mathrm{V,eff,1}} = 5534.5 \text{ KN} \text{ OK!!}$$

- <u>Block tearing (plate):</u> EC3-1-8, section 3.10 (CEN, 2005b)

$$A_{\mathrm{nt}} = 30.0\left(75.0 - \frac{33.0}{2}\right) = 1755.0 \text{ mm}^2$$

$$A_{\mathrm{nv}} = 30.0(1140.0 - 40.0 - (16.0 - 0.5) \times 33.0) = 17655.0 \text{ mm}^2$$

$$n_1 = 16.0 \text{ (number of bolts)}$$

$$V_{\mathrm{eff,1,Rd}} = \frac{490 \times 10^3 \times 1755 \times 10^{-6}}{1.25} + \frac{\frac{1}{\sqrt{3}} \times 355 \times 10^3 \times 17655 \times 10^{-6}}{1.0} = 4306.5 \text{ KN}$$

$$F_{\mathrm{V,Ed}} = 3600 \text{ KN} \leq F_{\mathrm{V,eff,1}} = 4306.5 \text{ KN} \text{ OK!!}$$

In this verification, the ductility criteria, for plastic analysis is achieved, being the block tearing of the gusset plate, the failure component, as demonstrated on table 41.

Failure mode	Resistance forces (KN)
Slip resistance (pre-stressed bolts)	4576.0
Bearing resistance (flange)	$3688.0 \times 4_{flanges} = 14752.0$
Net cross-section resistance (flange)	$1163.0 \times 4_{flanges} = 4652.0$
Block tearing (flange)	$5534.5 \times 4_{flanges} = 22138.0$
Block tearing (plate)	4306.5

Table 41: Failure modes of braces connections.

ANNEX A.2

On Annex A.2, a numerical analysis of transition element components by plastic criteria is performed. The first component to be studied is the flange of CHS 559 x 32mm. The design load is N_{ed} = 12700.0 KN (see figure 14).

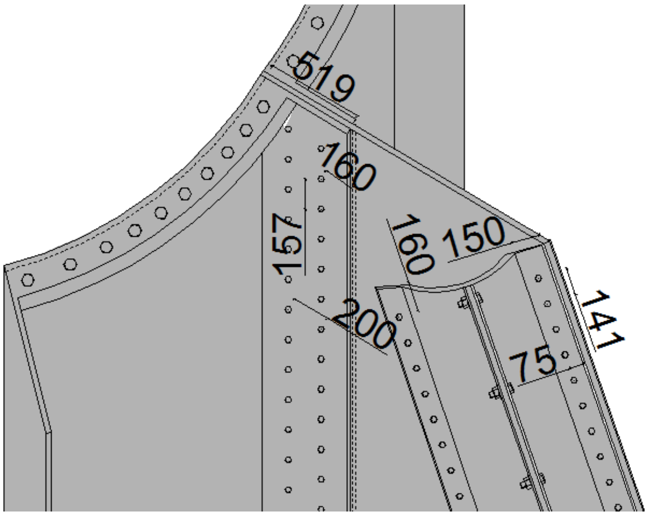

Figure 35: Spacing and edge distance of transition element

Spacing and edge distance (flange) – EC3-1-8, section 3.5	
e_1 (mm)	160.0
e_2 (mm)	75.0
p_1 (mm)	141.0

Table 42: Spacing and edge distance – flange CHS 559 x 32mm.

t_p (mm)	10.0
$h_{p,\ widht}$ (mm)	150.0
$h_{p,\ length}$(mm)	5646.6

Table 43: Geometry properties of flange CHS 559 x 32mm.

t_p (mm)	30.0
$h_{p\ length}$ (mm)	5646.0

Table 44: Geometry property of gusset plate.

Spacing and edge distance (gusset plate) – EC3-1-8, section 3.5	
e_1 (mm)	160.0
e_2 (mm)	75.0
p_1 (mm)	141.0
p_2 (mm)	709.0

Table 45: Spacing and edge distance – gusset plate (CHS 559 x 32mm).

➢ Slip resistance (criteria $F_{v,Ed} \leq F_{s,Rd}$): EC3-1-8, section 3.9.1 (CEN, 2005b)

$$F_{p,Cd} = 0.7 \times 1000.0 \times 10^3 \times \frac{561.0 \times 10^{-6}}{1.1} = 357.0 \text{ KN (design preloaded)}$$

$$F_{s,Rd} = \frac{K_s\ \eta\ \mu}{\gamma_{M3}} F_{P,c}$$

where, K_s is the coefficients for normal hole ($K_s = 1.00$);

η is the number of friction surface (see figure 24);

μ is the slip factor ($\mu = 0.50$);

$$F_{s,Rd} = \frac{1.0 \times 2 \times 0.5}{1.25} \times 357.0 = 285.6 \text{ KN (one bolt)}$$

The slip resistance of one pre-stressed bolt is 285.6 KN; exist seventy pre-stressed bolts linking the flanges with gusset plate (n = 70 pre-stressed bolts).

$$F_{s,Rd\ total} = 285.6 \times 70 = 19992.0 \text{ KN}$$

$$F_{V,Ed} = 12700.0 \text{ KN} \leq F_{s,Rd} = 19992.0 \text{ KN OK!!}$$

➢ Bearing resistance (criteria $F_{v,Ed} \leq F_{b,Rd}$):

$$F_{b,Rd} = \frac{k_1\ \alpha_b\ f_u\ d\ t}{\gamma_{M2}}$$

where, $\alpha_b = \min.(\alpha_d; \frac{f_{ub}}{f_u}; 1.0)$

$$\alpha_b = \min.\left(1.2; \frac{1000}{490} = 2.0; 1.0\right) = 1.0$$

<u>in the direction of load transfer</u>:

for end bolts $\alpha_d = \frac{e_1}{3d_0}$; for inner bolts $\alpha_d = \frac{p_1}{3d_0} - \frac{1}{4}$:

$$\alpha_d = \frac{160.0}{3 \times 33.0} = 1.6; \qquad \alpha_d = \frac{141.0}{3 \times 33.0} - \frac{1}{4} = 1.2$$

<u>perpendicular to the direction of load transfer</u>:

- for edge bolts:

$$k_1 = \text{minimum}\left(2.8\frac{e_2}{d_0} - 1.7;\ 2.5\right) = \min.\left(2.8 \times \frac{75.0}{33.0} - 1.70 = 4.7; 2.5\right) = 2.5$$

- for inner bolts:

$$k_1 = minimum\left(1.4\ \frac{p_2}{d_0} - 1.7;\ 2.5\right) = \min.\left(1.4 \times \frac{0}{33.0} - 1.7 = 0;\ 2.5\right) = 2.5$$

$$F_{b,Rd} = \frac{2.5 \times 1.0 \times 490.0 * 10^3 \times 30.0 \times 10^{-3} \times 10.0 \times 10^{-3}}{1.25} = \frac{368.0}{1.25} = 294.0\ \text{KN}$$

The bearing resistance of one pre-stressed bolt is 294.0 KN; exist thirty five pre-stressed bolts linking each flange (n = 35 pre-stressed bolts).

$$F_{b,Rd\ total} = 294.0 \times 35 = 10290.0\ \text{KN}$$

$$F_{V,Ed} = 3150.0\ \text{KN} \leq F_{b,Rd} = 10290.0\ \text{KN}\ \ \text{OK!!}$$

- <u>Resistance of net cross-section of flange (criteria $F_{v,Ed} \leq N_{net,Rd}$)</u> : EC3-1-1, section 6; (CEN, 2005a)

$$V_{net,Rd} = \frac{A_{net}\, f_{up}}{\sqrt{3} \times \gamma_{M2}}$$

$$A_{v,net} = h_p * t_p - n \times d_0 \times t_p = 5646.6 \times 10.0 - 35 \times 33.0 \times 10.0 = 44916.0\ mm^2$$

n = 35 (number of bolts)

$$V_{net,Rd} = \frac{44916.0 \times 10^{-6} \times 490.0 \times 10^3}{\sqrt{3} \times 1.25} = 10165.5\ KN$$

$$F_{V,Ed} = 3175.0\ KN \leq N_{net,Rd} = 10165.5\ KN \ \ OK!!$$

So far, the verifications are dedicated for the flanges, due its fragility. Next, is verified the block tearing where are studied both components, flange and plate.

- <u>Block tearing (flange):</u> EC3-1-8, section 3.10 (CEN, 2005b)

$$V_{eff,2,Rd} = 0.5 \times \frac{f_u A_{nt}}{\gamma_{M2}} + \frac{\frac{1}{\sqrt{3}} f_y A_{nv}}{\gamma_{M0}}$$

$$A_{nt} = t_p\left(e_2 - \frac{d_0}{2}\right)$$

$$A_{nt} = 10.0\left(75.0 - \frac{33.0}{2}\right) = 585.0\ mm^2$$

$$A_{nv} = t_p\big(h_p - e_1 - (n_1 - 0.5) \times d_0\big)$$

$$A_{nv} = 10.0 \times (5646.6 - 160.0 - (35.0 - 0.5) \times 33.0) = 43481.0\ mm^2$$

$n_1 = 35.0$ (nº of bolts)

$$V_{eff,2,Rd} = 0.5 \times \frac{490 \times 10^3 \times 585 \times 10^{-6}}{1.25} + \frac{\frac{1}{\sqrt{3}} \times 355 \times 10^3 \times 43481 \times 10^{-6}}{1.0}$$
$$= 8642.2\ KN$$

$$F_{V,Ed} = 3175.0\ KN \leq F_{V,eff,1} = 8642.2\ KN \ \ OK!!$$

➢ Block tearing (plate): EC3-1-8, section 3.10 (CEN, 2005b)

$$A_{nt} = 30.0\left(75.0 - \frac{33.0}{2}\right) = 1755.0\ mm^2$$

$$A_{nv} = 30.0(5646.6 - 160.0 - (70.0 - 0.5) \times 33.0) = 95793.0\ mm^2$$

$$n_1 = 70.0 \text{ (number of bolts)}$$

$$V_{eff,2,Rd} = 0.5 \times \frac{490 \times 10^3 \times 1755 \times 10^{-6}}{1.25} + \frac{\frac{1}{\sqrt{3}} \times 355 \times 10^3 \times 95793 \times 10^{-6}}{1.0} = 19135.1KN$$

$$F_{V,Ed} = 12700.0\ KN \leq F_{V,eff,2} = 19135.1\ KN\ \ OK!!$$

On this verification the ductility criteria, for plastic analysis is achieved, being the block tearing of the gusset plate the failure component, as demonstrate on table 46.

Failure mode	Resistance forces (KN)
Slip resistance (pre-stressed bolts)	19992.0
Bearing resistance (flange)	$10290.0 \times 4_{flanges} = 41160.0$
Net cross-section resistance (flange)	$10165.5 \times 4_{flanges} = 40662.0$
Block tearing (flange)	$8642.2 \times 4_{flanges} = 34568.8$
Block tearing (plate)	19135.1

Table 46: Failure modes of CHS 559 x 32mm.

Next is verified the safety of link among the flanges and the gusset plate, N_{ed} = 11510.0 KN.

Spacing and edge distance (flange) – EC3-1-8, section 3.5	
e_1 (mm)	160.0
e_2 (mm)	160.0
p_1 (mm)	157.0
p_2 (mm)	200.0

Table 47: Spacing and edge distance – flange transition piece.

t_p (mm)	20.0
$h_{p,\ widht}$ (mm)	520.0
$h_{p,\ length}$(mm)	4560.0

Table 48: Geometry properties of flange CHS 559 x 32mm.

t_p (mm)	30.0
$h_{p\ length}$ (mm)	4560.0

Table 49: Geometry property of gusset plate.

Spacing and edge distance (gusset plate) – EC3-1-8, section 3.5	
e_1 (mm)	160.0
e_2 (mm)	160.0
p_1 (mm)	157.0
p_2 (mm)	200.0

Table 50: Spacing and edge distance – gusset plate transition piece.

➢ Slip resistance (criteria $F_{v,Ed} \leq F_{s,Rd}$): EC3-1-8, section 3.9.1 (CEN, 2005b)

$$F_{p,Cd} = 0.7 \times 1000.0 \times 10^3 \times \frac{561.0 \times 10^{-6}}{1.1} = 357.0 \text{ KN (design preloaded)}$$

$$F_{s,Rd} = \frac{K_s\ \eta\ \mu}{\gamma_{M3}} F_{P,c}$$

where, K_s is the coefficients for normal hole ($K_s = 1.00$);

η is the number of friction surface (see figure 24);

μ is the slip factor ($\mu = 0.50$);

$$F_{s,Rd} = \frac{1.0 \times 2 \times 0.5}{1.25} \times 357.0 = 285.6 \text{ KN (one bolt)}$$

The slip resistance of one pre-stressed bolt is 285.6 KN; exist fifty six pre-stressed bolts linking the flanges with gusset plate (n = 56 pre-stressed bolts).

$$F_{s,Rd\ total} = 285.6 \times 56 = 15993.6\ KN$$

$$F_{V,Ed} = 11510.0\ KN \leq F_{s,Rd} = 15993.6\ KN\ \ OK!!$$

- <u>Bearing resistance (criteria $F_{v,Ed} \leq F_{b,Rd}$)</u>:

$$F_{b,Rd} = \frac{k_1\ \alpha_b\ f_u\ d\ t}{\gamma_{M2}}$$

where, $\alpha_b = \min.(\alpha_d; \frac{f_{ub}}{f_u}; 1.0)$

$$\alpha_b = \min.\left(1.6; \frac{1000}{490} = 2.0; 1.0\right) = 1.0$$

<u>in the direction of load transfer</u>:

for end bolts $\alpha_d = \frac{e_1}{3d_0}$; for inner bolts $\alpha_d = \frac{p_1}{3d_0} - \frac{1}{4}$:

$$\alpha_d = \frac{160.0}{3 \times 33.0} = 1.6; \qquad \alpha_d = \frac{157.0}{3 \times 33.0} - \frac{1}{4} = 1.8$$

<u>perpendicular to the direction of load transfer</u>:

- for edge bolts:

$$k_1 = \text{minimum}\left(2.8\frac{e_2}{d_0} - 1.7;\ 2.5\right) = \min.\left(2.8 \times \frac{160.0}{33.0} - 1.70 = 11.9; 2.5\right) = 2.5$$

- for inner bolts:

$$k_1 = minimum\left(1.4\ \frac{p_2}{d_0} - 1.7;\ 2.5\right) = \min.\left(1.4 \times \frac{200.0}{33.0} - 1.7 = 6.8;\ 2.5\right) = 2.5$$

$$F_{b,Rd} = \frac{2.5 \times 1.0 \times 490.0 * 10^3 \times 30.0 \times 10^{-3} \times 20.0 \times 10^{-3}}{1.25} = \frac{735.0}{1.25} = 588.0\ KN$$

The bearing resistance of one pre-stressed bolt is 588.0 KN; exist fifty six pre-stressed bolts linking flanges and plate (n = 56 pre-stressed bolts).

$$F_{b,Rd\ total} = 588.0 \times 56 = 32928.0\ KN$$

$$F_{V,Ed} = 5755.0\ KN \leq F_{b,Rd} = 32928.0\ KN\ \ OK!!$$

➢ Resistance of net cross-section of flange (criteria $F_{v,Ed} \leq N_{net,Rd}$) : EC3-1-1, section 6;

$$V_{net,Rd} = \frac{A_{net}\, f_{up}}{\sqrt{3} \times \gamma_{M2}}$$

$$A_{v,net} = h_p * t_p - n \times d_0 \times t_p = 4560.0 \times 20.0 - 28 \times 33.0 \times 20.0 = 72720.0\ mm^2$$

n = 28 (number of bolts)

$$V_{net,Rd} = \frac{72720.0 \times 10^{-6} \times 490.0 \times 10^3}{\sqrt{3} \times 1.25} = 16460.0\ KN$$

$$F_{V,Ed} = 5755.0\ KN \leq N_{net,Rd} = 16460.0\ KN\ \ OK!!$$

So far, the verifications are dedicated for the flanges, due its fragility. Next, is verified the block tearing where are studied both components, flange and plate.

➢ Block tearing (flange): EC3-1-8, section 3.10 (CEN, 2005b)

$$V_{eff,2,Rd} = 0.5 \times \frac{f_u\, A_{nt}}{\gamma_{M2}} + \frac{\frac{1}{\sqrt{3}}\, f_y\, A_{nv}}{\gamma_{M0}}$$

$$A_{nt} = t_p \left(e_2 - \frac{d_0}{2}\right)$$

$$A_{nt} = 20.0\left(160.0 - \frac{33.0}{2}\right) = 2870.0\ mm^2$$

$$A_{nv} = t_p\left(h_p - e_1 - (n_1 - 0.5) \times d_0\right)$$

$$A_{nv} = 20.0 \times (4560.0 - 160.0 - (56.0 - 0.5) \times 33.0) = 51370.0\ mm^2$$

$n_1 = 56.0$ (n° of bolts)

$$V_{eff,2,Rd} = 0.5 \times \frac{490 \times 10^3 \times 2870 \times 10^{-6}}{1.25} + \frac{\frac{1}{\sqrt{3}} \times 355 \times 10^3 \times 51370 \times 10^{-6}}{1.0}$$
$$= 10656.8 \text{ KN}$$

$$F_{V,Ed} = 5755.0 \text{ KN} \leq F_{V,eff,2} = 10656.8 \text{ KN OK!!}$$

- <u>Block tearing (plate):</u> EC3-1-8, section 3.10 (CEN, 2005b)

$$A_{nt} = 30.0\left(160.0 - \frac{33.0}{2}\right) = 4305.0 \text{ mm}^2$$

$$A_{nv} = 30.0(4560.0 - 160.0 - (56.0 - 0.5) \times 33.0) = 77055.0 \text{ mm}^2$$

$n_1 = 56.0$ (number of bolts)

$$V_{eff,2,Rd} = 0.5 \times \frac{490 \times 10^3 \times 4305 \times 10^{-6}}{1.25} + \frac{\frac{1}{\sqrt{3}} \times 355 \times 10^3 \times 77055 \times 10^{-6}}{1.0}$$
$$= 15985.1 \text{ KN}$$

$$F_{V,Ed} = 11510.0 \text{ KN} \leq F_{V,eff,2} = 15985.1 \text{ KN OK!!}$$

On this verification the ductility criteria, for plastic analysis is achieved, being the block tearing of the gusset plate the failure component, as demonstrate on table 51.

Failure mode	Resistance forces (KN)
Slip resistance (pre-stressed bolts)	15993.6
Bearing resistance (flange)	$32928.0 \times 4_{flanges} = 131712.0$
Net cross-section resistance (flange)	$16460.0 \times 4_{flanges} = 65840.0$
Block tearing (flange)	$10656.8 \times 4_{flanges} = 42627.2$
Block tearing (plate)	15985.1

Table 51: Failure modes of flanges transition element.

ANNEX B.1

Pad foundation quick design: N_{ed} = 7600.0 KN (Support reaction); 25/30 MPa; rígid foundation;

Top segment:

$$0.6 \times \sigma_c = \frac{N_{Ed}}{A} => A = \frac{N_{Ed}}{0.6 \times \sigma_C} = \frac{7600.0}{0.6 \times \frac{25.0}{1.5}} = 0.8\ m^2 => A_{adopted} = 1.0 \times 1.0 = 1.0 m^2$$

Bottom segment:

$\sigma_{ref.}$ = 304.0 KN

Effective depth: Alonso $d \geq \begin{cases} \frac{5.0-1.0}{4} = 1.0 \\ \frac{5.0-1.0}{4} = 1.0 \\ 1.44 \times \sqrt{\frac{7600.0}{0.85 \times \frac{25000}{1.96}}} = 1.21 \end{cases}$; d = 1.44m

Overall depth = 1.44 + 0.06 = 1.50m

$$A_u = (1 + 1.44) \times (1.0 + 1.44) - \left(\frac{4 - \pi}{4}\right) \times 1.44^2 = 5.51 m^2$$

$$u = 2 \times (1.0 + 1.0) + \pi \times 1.44 = 8.52 m$$

$$N_{Sd,0} = \frac{\frac{7600.0}{1.35}}{5.0 \times 5.0} = 225.0\ KPa$$

$$\Delta V_{Sd} = 225.0 \times 5.51 = 1240\ KN$$

$$V_{Sd,red.} = N_{Sd} - \Delta V_{sd} = 7600.0 - 1240.0 = 6360.0\ KN$$

$$V_{Sd} = \frac{6360.0}{8.5 \times 1.44} = 518.0\ KPa \leq \tau 1 = 750.0\ KPa \quad OK!!$$